DRAFT VERSION OCTOBER 6, 2017
Typeset using LaTeX **twocolumn** style in AASTeX61

MULTI-MESSENGER OBSERVATIONS OF A BINARY NEUTRON STAR MERGER

LIGO SCIENTIFIC COLLABORATION, VIRGO COLLABORATION AND PARTNER ASTRONOMY GROUPS

(Dated: October 6, 2017)

ABSTRACT

On August 17, 2017 a binary neutron star coalescence candidate (later designated GW170817) with merger time 12:41:04 UTC was observed through gravitational waves by the Advanced LIGO and Advanced Virgo detectors. The *Fermi* Gamma-ray Burst Monitor independently detected a gamma-ray burst (GRB170817A) with a time-delay of $\sim 1.7\,\mathrm{s}$ with respect to the merger time. From the gravitational-wave signal, the source was initially localized to a sky region of $31\,\mathrm{deg}^2$ at a luminosity distance of $40^{+8}_{-8}\,\mathrm{Mpc}$ and with component masses consistent with neutron stars. The component masses were later measured to be in the range 0.86 to 2.26 $M_\odot$. An extensive observing campaign was launched across the electromagnetic spectrum leading to the discovery of a bright optical transient (SSS17a, now with the IAU identification of AT2017gfo) in NGC 4993 (at $\sim 40\,\mathrm{Mpc}$) less than 11 hours after the merger by the One-Meter, Two Hemisphere (1M2H) team using the 1-m Swope Telescope. The optical transient was independently detected by multiple teams within an hour. Subsequent observations targeted the object and its environment. Early ultraviolet observations revealed a blue transient that faded within 48 hours. Optical and infrared observations showed a redward evolution over ~ 10 days. Following early non-detections, X-ray and radio emission were discovered at the transient's position $\sim$9 and $\sim$16 days, respectively, after the merger. Both the X-ray and radio emission likely arise from a physical process that is distinct from the one that generates the UV/optical/near-infrared emission. No ultra-high-energy gamma rays and no neutrino candidates consistent with the source were found in follow-up searches. These observations support the hypothesis that GW170817 was produced by the merger of two neutron stars in NGC 4993 followed by a short gamma-ray burst (GRB170817A) and a kilonova/macronova powered by the radioactive decay of r-process nuclei synthesized in the ejecta.

1. INTRODUCTION

Over 80 years ago Baade & Zwicky (1934) proposed the idea of neutron stars, and soon after, Oppenheimer & Volkoff (1939) carried out the first calculations of neutron-star models. Neutron stars entered the realm of observational astronomy in the 1960s, by providing a physical interpretation of X-ray emission from Scorpius X-1 (Giacconi et al. 1962; Shklovsky 1967) and of radio pulsars (Hewish et al. 1968; Gold 1968, 1969).

The discovery of a radio pulsar in a double neutron-star system by Hulse & Taylor (1975) led to a renewed interest in binary stars and compact-object astrophysics, including the development of a scenario for the formation of double neutron stars and the first population studies (Flannery & van den Heuvel 1975; Massevitch et al. 1976; Clark 1979; Clark et al. 1979; Lipunov et al. 1987; Dewey & Cordes 1987; for reviews see Kalogera et al. 2007; Postnov & Yungelson 2014). The Hulse-Taylor pulsar provided the first firm evidence (Taylor & Weisberg 1982) for the existence of gravitational waves (Einstein 1916, 1918), and sparked a renaissance of observational tests of general relativity (Damour & Taylor 1991; Taylor et al. 1992; Damour & Taylor 1992; Wex 2014). Merging binary neutron stars were quickly recognized to be promising sources of detectable gravitational waves, making them a primary target for ground-based interferometric detectors (see Abadie et al. 2010, for an overview). This motivated the development of accurate models for the two-body, general-relativistic dynamics (Blanchet et al. 1995; Buonanno & Damour 1999; Pretorius 2005; Campanelli et al. 2006; Baker et al. 2006; Blanchet 2014) that are critical for detecting and interpreting gravitational waves (Abbott et al. 2016a,b, 2017a,b,c).

In the mid-1960s gamma-ray bursts (GRBs) were discovered by the Vela satellites, and their cosmic origin was first established by Klebesadel et al. (1973). GRBs are classified as *long* or *short*, based on their duration and spectral hardness (Dezalay et al. 1992; Kouveliotou et al. 1993). Uncovering the progenitors of GRBs has been one of the key challenges in high-energy astrophysics ever since (Lee & Ramirez-Ruiz 2007). It has long been suggested that short GRBs might be related to neutron-star mergers (Paczynski 1986; Goodman 1986; Eichler et al. 1989; Narayan et al. 1992).

In 2005 the field of short gamma-ray burst (sGRB) studies experienced a breakthrough (for reviews see Nakar 2007; Berger 2014) with the identification of the first host galaxies of sGRBs and multi-wavelength observation (from X-ray to optical and radio) of their afterglows (Gehrels et al. 2005; Fox et al. 2005a; Villasenor et al. 2005; Hjorth et al. 2005a; Berger et al. 2005). These observations provided strong hints that sGRBs might be associated with mergers of neutron stars with other neutron stars or with black holes. These hints included: (i) their association with both elliptical and star forming galaxies (Barthelmy et al. 2005; Prochaska et al. 2006; Berger et al. 2007; Ofek et al. 2007; Troja et al. 2008; D'Avanzo et al. 2009; Fong et al. 2013), due to a very wide range of delay times, as predicted theoretically (Bagot et al. 1998; Fryer et al. 1999; Belczynski et al. 2002); (ii) a broad distribution of spatial offsets from host-galaxy centers (Berger 2010; Fong & Berger 2013; Tunnicliffe et al. 2014),which was predicted to arise from supernova kicks (Narayan et al. 1992; Bloom et al. 1999); and (iii) the absence of associated supernovae (Fox et al. 2005b; Hjorth et al. 2005b,c; Soderberg et al. 2006; Kocevski et al. 2010; Berger et al. 2013a). Despite these strong hints, proof that sGRBs were powered by neutron-star mergers remained elusive, and interest intensified in following up gravitational-wave detections electromagnetically (Metzger & Berger 2012; Nissanke et al. 2013).

Evidence of beaming in some sGRBs was initially found by Soderberg et al. (2006); Burrows et al. (2006) and confirmed by subsequent sGRB discoveries (see compilation and analysis by Fong et al. 2015 and also Troja et al. 2016). Neutron-star binary mergers are also expected, however, to produce isotropic electromagnetic signals, which include: (i) early optical and infrared emission, a so-called kilonova/macronova (hereafter kilonova) (Li & Paczyński 1998; Kulkarni 2005; Rosswog 2005; Metzger et al. 2010; Roberts et al. 2011; Kasen et al. 2013; Barnes & Kasen 2013; Tanaka & Hotokezaka 2013; Grossman et al. 2014; Barnes et al. 2016; Tanaka 2016; Metzger 2017) due to radioactive decay of rapid neutron-capture process (r-process) nuclei (Lattimer & Schramm 1974, 1976) synthesized in dynamical and accretion-disk-wind ejecta during the merger; and (ii) delayed radio emission from the interaction of the merger ejecta with the ambient medium (Nakar & Piran 2011; Piran et al. 2013; Hotokezaka & Piran 2015; Hotokezaka et al. 2016). The late-time infrared excess associated with GRB130603B was interpreted as the signature of r-process nucleosynthesis (Berger et al. 2013b; Tanvir et al. 2013), and more candidates were identified later (for a compilation see Jin et al. 2016).

Here we report on the global effort[1] that led to the first joint detection of gravitational and electromagnetic radiation from a single source. A ~ 100 s-long gravitational-wave signal (GW170817) was followed by a sGRB (GRB170817A) and an optical transient (SSS17a/AT2017gfo) found in the host galaxy NGC 4993. The source was detected across the electromagnetic spectrum – in the X-ray, ultraviolet, optical, infrared, and radio bands – over hours, days, and weeks. These

[1] This effort was established in the time between initial and advanced LIGO-Virgo observations. Partners have followed up binary-black-hole detections, starting with GW150914 Abbott et al. 2016, but have discovered no firm electro-magnetic counterparts to those events.

observations support the hypothesis that GW170817 was produced by the merger of two neutron stars in NGC4993, followed by a sGRB and a kilonova powered by the radioactive decay of r-process nuclei synthesized in the ejecta.

2. A MULTI-MESSENGER TRANSIENT

On August 17, 2017 12:41:06 UTC the *Fermi* Gamma-ray Burst Monitor (GBM) (Meegan et al. 2009) on-board flight software triggered on, classified, and localized, a GRB. A Gamma-ray Coordinates Network (GCN) Notice (Fermi-GBM 2017) was issued at 12:41:20 UTC announcing the detection of the GRB, which was later designated GRB170817A (von Kienlin et al. 2017). Approximately 6 minutes later, a gravitational-wave candidate (later designated GW170817) was registered in low latency (Cannon et al. 2012; Messick et al. 2017) based on a single-detector analysis of the Laser Interferometer Gravitational-wave Observatory (LIGO) Hanford data. The signal was consistent with a BNS coalescence with merger time, t_c, 12:41:04 UTC, less than 2 s before GRB170817A. Single-detector gravitational-wave triggers had never been disseminated before in low-latency. Given the temporal coincidence with the *Fermi*-GBM GRB, however, a GCN Circular was issued at 13:21:42 UTC (The LIGO Scientific Collaboration et al. 2017a) reporting that a highly significant candidate event consistent with a BNS coalescence was associated with the time of the GRB[2]. An extensive observing campaign was launched across the electromagnetic spectrum in response to the *Fermi*-GBM and LIGO-Virgo detections, and especially the well-constrained, three-dimensional LIGO-Virgo localization. A bright optical transient (SSS17a, now with the IAU identification of AT2017gfo) was discovered in NGC 4993 (at ~ 40 Mpc) by the One-Meter, Two Hemisphere (1M2H) team (August 18 01:05 UTC; Coulter et al. 2017a) less than 11 hr after the merger.

2.1. *Gravitational Wave Observation*

GW170817 was first detected online (Cannon et al. 2012; Messick et al. 2017) as a single-detector trigger and disseminated through a GCN Circular at 13:21:42 UTC (The LIGO Scientific Collaboration et al. 2017a). A rapid reanalysis (Nitz et al. 2017a,b) of data from LIGO-Hanford, LIGO-Livingston and Virgo confirmed a highly significant, coincident signal. These data were then combined to produce the first three-instrument sky map (Singer & Price 2016; Singer et al. 2016) at 17:54:51 UTC (The LIGO Scientific Collaboration et al. 2017b), placing the source nearby, at a luminosity distance *initially* estimated to be 40^{+8}_{-8} Mpc, in an elongated region of ≈ 31 deg^2 (90% credibility), centered around right ascension $\alpha(\mathrm{J2000.0}) = 12\mathrm{h}57^{\mathrm{m}}$ and declination $\delta(\mathrm{J2000.0}) = -17°51'$. Soon after, a coherent analysis (Veitch et al. 2015) of the data from the detector network produced a sky map that was distributed at 23:54:40 UTC (The LIGO Scientific Collaboration et al. 2017c), consistent with the initial one: a $\simeq 34$ deg^2 sky region at 90% credibility centered around $\alpha(\mathrm{J2000.0}) = 13\mathrm{h}09^{\mathrm{m}}$ and $\delta(\mathrm{J2000.0}) = -25°37'$

The offline gravitational-wave analysis of the LIGO-Hanford and LIGO-Livingston data identified GW170817 with a false-alarm-rate of less than one per 8.0×10^4 years (Abbott et al. 2017c). This analysis uses post-Newtonian waveform models (Blanchet et al. 1995, 2004, 2006; Bohé et al. 2013) to construct a matched-filter search (Sathyaprakash & Dhurandhar 1991; Cutler et al. 1993; Allen et al. 2012) for gravitational waves from the coalescence of compact-object binary systems in the (detector frame) total mass range $2 - 500\,M_\odot$. GW170817 lasted for ~ 100 seconds in the detector sensitivity band. The signal reached Virgo first, then LIGO-Livingston 22 ms later, and after 3 ms more, it arrived at LIGO-Hanford. GW170817 was detected with a combined signal-to-noise ratio across the three-instrument network of 32.4. For comparison, GW150914 was observed with a signal-to-noise ratio of 24 (Abbott et al. 2016a).

The properties of the source that generated GW170817 (see Abbott et al. 2017c for full details; here we report parameter ranges that span the 90% credible interval) were derived by employing a coherent Bayesian analysis (Veitch et al. 2015; Abbott et al. 2016) of the three-instrument data, including marginalisation over calibration uncertainties and assuming that the signal is described by waveform models of a binary system of compact objects in quasi-circular orbits (see Abbott et al. 2017c and references therein). The waveform models include the effects introduced by the objects' intrinsic rotation (spin) and tides. The source is located in a region of 28 deg^2 at a distance 40^{+8}_{-14} Mpc, see Fig. 1, consistent with the early estimates disseminated through GCN Circulars (The LIGO Scientific Collaboration et al. 2017b,c). The misalignment between the total angular momentum axis and the line of sight is $\leq 56°$.

The (source-frame[3]) masses of the primary and secondary components, m_1 and m_2, respectively, are in the range $m_1 \in (1.36 - 2.26)M_\odot$ and $m_2 \in (0.86 - 1.36)\,M_\odot$. The chirp

[2] The trigger was recorded with LIGO-Virgo ID G298048, to which it is referred throughout the GCN circulars.

[3] Any mass parameter $m^{(\mathrm{det})}$ derived from the observed signal is measured in the detector frame. It is related to the mass parameter, m, in the source-frame by $m^{(\mathrm{det})} = (1+z)m$, where z is the source's redshift. Here we always report source-frame mass parameters, assuming standard cosmology (Ade et al. 2016) and correcting for the motion of the Solar System Barycenter with respect to the Cosmic Microwave Background (Fixsen 2009). From the gravitational-wave luminosity distance measurement, the redshift is determined to be $z = 0.008^{+0.002}_{-0.003}$. For full details see (Abbott et al. 2016, 2017c; The LIGO Scientific Collaboration et al. 2017d).

mass[4], $\mathcal{M}$, is the mass parameter that, at the leading order, drives the frequency evolution of gravitational radiation in the inspiral phase. This dominates the portion of GW170817 in the instruments' sensitivity band. As a consequence, it is the best measured mass parameter, $\mathcal{M} = 1.188^{+0.004}_{-0.002}\,M_\odot$. The total mass is $2.82^{+0.47}_{-0.09}\,\mathrm{M}_\odot$, and the mass ratio m_2/m_1 is bound to the range $0.4 - 1.0$. These results are consistent with a binary whose components are neutron stars. White dwarfs are ruled out since the gravitational-wave signal sweeps through 200 Hz in the instruments' sensitivity band, implying an orbit of size ~ 100 km, which is smaller than the typical radius of a white dwarf by an order of magnitude (Shapiro & Teukolsky 1983). However, for this event gravitational-wave data *alone* cannot rule out objects more compact than neutron stars such as quark stars or black holes (Abbott et al. 2017c).

2.2. *Prompt Gamma-Ray Burst Detection*

The first announcement of GRB170817A came from the GCN Notice (Fermi-GBM 2017) automatically-generated by *Fermi*-GBM at 12:41:20 UTC, just 14 s after the detection of the GRB at T0 = 12:41:06 UTC. GRB170817A was later detected by the International Gamma-Ray Astrophysics Laboratory (INTEGRAL) spacecraft using the anti-coincidence shield (von Kienlin et al. 2003) of the Spectrometer onboard INTEGRAL (SPI), through an offline search initiated by the LIGO-Virgo and *Fermi*-GBM reports. The final *Fermi*-GBM localization constrained GRB170817A to a region with highest probability at $\alpha(\mathrm{J2000.0}) = 12\mathrm{h}28^\mathrm{m}$ and $\delta(\mathrm{J2000.0}) = -30^\circ$ and 90% probability region covering $\sim$1100 deg^2 (Goldstein et al. 2017). The difference between the binary merger and the GRB is $\mathrm{T0} - t_c = 1.734 \pm 0.054$ s (LIGO Scientific and Virgo Collaboration et al. 2017). Exploiting the difference in the arrival time of the gamma-ray signals at *Fermi*-GBM and INTEGRAL SPI-ACS (Svinkin et al. 2017) provides additional significant constraints on the gamma-ray localization area (see Figure 1). The IPN localization capability will be especially important in the case of future gravitational-wave events that might be less-well localized by LIGO-Virgo.

Standard follow-up analyses (Paciesas et al. 2012; Goldstein et al. 2012; Gruber et al. 2014) of the *Fermi*-GBM trigger determined the burst duration to be $T_{90} = 2.0 \pm 0.5$ s, where T_{90} is defined as the interval over which 90% of the burst fluence is accumulated in the energy range of 50–300 keV. From the *Fermi*-GBM T_{90} measurement, GRB170817A was classified as a sGRB with 3:1 odds over being a long GRB. The classification of GRB170817A as a sGRB is further supported by incorporating the hardness ratio of the burst and comparing it to the *Fermi*-GBM catalog (Goldstein et al. 2017). The SPI-ACS duration for GRB170817A of 100 ms is consistent with a sGRB classification within the instrument's historic sample (Savchenko et al. 2012).

The GRB had a peak photon flux measured on a 64 ms timescale of 3.7 ± 0.9 photons s^{-1} cm^{-2} and a fluence over the T_{90} interval of $(2.8 \pm 0.2) \times 10^{-7}$ erg cm^{-2} (10–1000 keV) (Goldstein et al. 2017). GRB170817A is the closest sGRB with measured redshift. By usual measures, GRB170817A is sub-luminous, a tantalizing observational result that is explored in LIGO Scientific and Virgo Collaboration et al. (2017); Goldstein et al. (2017).

Detailed analysis of the *Fermi*-GBM data for GRB170817A revealed two components to the burst: a main pulse encompassing the GRB trigger time from $\mathrm{T0} - 0.320$ s to $\mathrm{T0} + 0.256$ s followed by a weak tail starting at $\mathrm{T0} + 0.832$ s and extending to $\mathrm{T0} + 1.984$ s. The spectrum of the main pulse of GRB170817A is best-fit with a Comptonized function (a power-law with an exponential cutoff) with a power-law photon index of -0.62 ± 0.40, peak energy $E_\mathrm{peak} = 185 \pm 62$ keV, and time-averaged flux of $(3.1 \pm 0.7) \times 10^{-7}$ erg cm^{-2} s^{-1}. The weak tail that follows the main pulse, when analyzed independently, has a localization consistent with both the main pulse and the gravitational-wave position. The weak tail, at 34% the fluence of the main pulse, extends the T_{90} beyond the main pulse and has a softer, blackbody spectrum with $kT = 10.3 \pm 1.5$ keV (Goldstein et al. 2017).

Using the *Fermi*-GBM spectral parameters of the main peak and T_{90} interval, the integrated fluence measured by INTEGRAL SPI-ACS is $(1.4 \pm 0.4) \times 10^{-7}$ erg cm^{-2} (75–2000 keV), compatible with the *Fermi*-GBM spectrum. Because SPI-ACS is most sensitive above 100 keV, it detects only the highest-energy part of the main peak near the start of the longer *Fermi*-GBM signal (The LIGO Scientific Collaboration et al. 2017e).

2.3. *Discovery of Optical Counterpart and Host Galaxy*

The announcements of the *Fermi*-GBM and LIGO-Virgo detections, and especially the well-constrained, three-dimensional LIGO-Virgo localization, triggered a broadband observing campaign in search of electromagnetic counterparts. A large number of teams across the world were mobilized using ground- and space-based telescopes that could observe the region identified by the gravitational-wave detection. GW170817 was localized to the southern sky, setting in the early evening for the northern hemisphere telescopes, thus making it inaccessible to the majority of them. The LIGO-Virgo localization region (The LIGO Scientific Collaboration et al. 2017b,c) became observable to telescopes in

[4] The binary's chirp mass is defined as $\mathcal{M} = (m_1 m_2)^{3/5}/(m_1 + m_2)^{1/5}$.

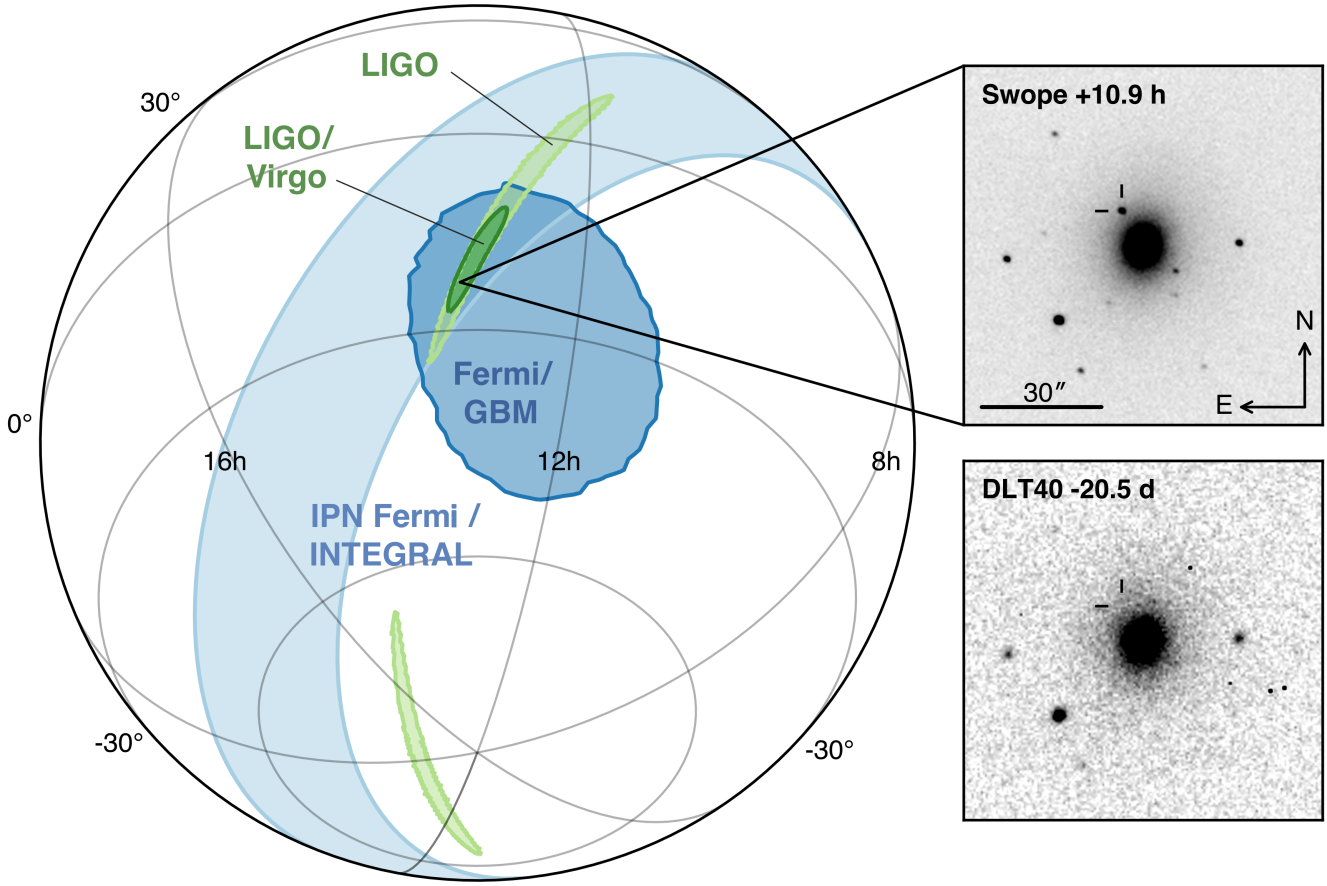

Figure 1. Localization of the gravitational-wave, gamma-ray, and optical signals. The left panel shows an orthographic projection of the 90% credible regions from LIGO (190 deg^2, light green), the initial LIGO-Virgo localization (31 deg^2, dark green), IPN triangulation from the time delay between *Fermi* and *INTEGRAL* (light blue), and *Fermi* GBM (dark blue). The inset shows the location of the apparent host galaxy NGC 4993 in the Swope optical discovery image at 10.9 hours after the merger (top right) and the DLT40 pre-discovery image from 20.5 days prior to merger (bottom right). The reticle marks the position of the transient in both images.

Chile about 10 hours after the merger with an altitude above the horizon of about 45 degrees.

The One-Meter, Two-Hemisphere (1M2H) team was the first to discover and announce (Aug 18 01:05 UTC; Coulter et al. 2017a) a bright optical transient in an i-band image acquired on Aug 17 at 23:33 UTC (t_c+10.87 hr) with the 1 m Swope telescope at Las Campanas Observatory in Chile. The team used an observing strategy (Gehrels et al. 2016) that targeted known galaxies (from White et al. 2011) in the three-dimensional LIGO-Virgo localization taking into account the galaxy stellar mass and star-formation rate (Coulter et al. 2017). The transient, designated Swope Supernova Survey 2017a (SSS17a), was $i = 17.057 \pm 0.018$ mag[5] (Aug 17 23:33 UTC, t_c+10.87 hr) and did not match any known asteroids or supernovae. SSS17a (now with the IAU designation AT2017gfo) was located at $\alpha(\mathrm{J2000.0}) = 13^{\mathrm{h}}09^{\mathrm{m}}48^{\mathrm{s}}.085 \pm 0.018$, $\delta(\mathrm{J2000.0}) = -23°22'53''.343 \pm 0.218$ at a projected distance of $10.6''$ from the center of NGC 4993, an early-type galaxy in the ESO 508 group at a distance of $\simeq 40$ Mpc (Tully-Fisher distance from Freedman et al. 2001), consistent with the gravitational-wave luminosity distance (The LIGO Scientific Collaboration et al. 2017b).

Five other teams took images of the transient within an hour of the 1M2H image (and before the SSS17a announcement) using different observational strategies to search the LIGO-Virgo sky localization region. They reported their discovery of the same optical transient in a sequence of GCNs: the Dark Energy Camera (01:15 UTC; Allam et al. 2017), the Distance Less Than 40 Mpc survey (01:41 UTC; Yang et al. 2017a), Las Cumbres Observatory (04:07 UTC; Arcavi et al. 2017a), the Visible and Infrared Survey Telescope for Astronomy (05:04 UTC; Tanvir et al. 2017a), and MASTER (05:38 UTC; Lipunov et al. 2017a). Independent searches were also carried out by the Rapid Eye Mount (REM-GRAWITA, optical, 02:00 UTC; Melandri et al. 2017a), Swift UVOT/XRT (utraviolet, 07:24 UTC;

[5] All apparent magnitudes are AB and corrected for the Galactic extinction in the direction of SSS17a ($E(B-V) = 0.109$ mag; Schlafly & Finkbeiner 2011).

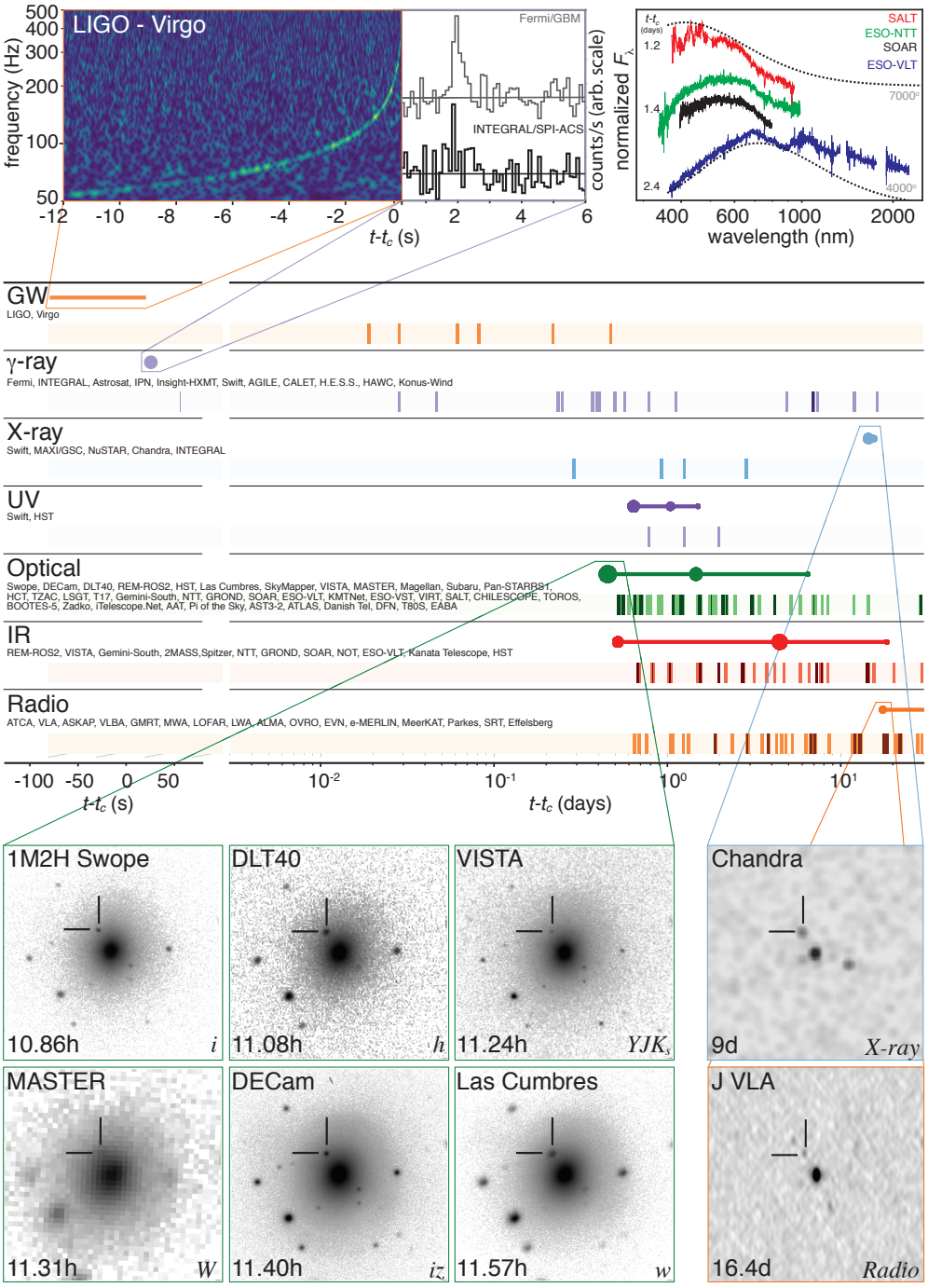

Figure 2. The timeline of the discovery of GW170817, GRB170817A, SSS17a/AT 2017gfo and the follow-up observations are shown by messenger and wavelength relative to the time t_c of the gravitational-wave event. Two types of information are shown for each band/messenger. First, the shaded dashes represent the times when information was reported in a GCN Circular. The names of the relevant instruments, facilities or observing teams are collected at the beginning of the row. Second, representative observations (see Table 1) in each band are shown as solid circles with their areas approximately scaled by brightness; the solid lines indicate when the source was detectable by at least one telescope. Magnification insets give a picture of the first detections in the gravitational-wave, gamma-ray, optical, X-ray and radio bands. They are respectively illustrated by the combined spectrogram of the signals received by LIGO-Hanford and LIGO-Livingston (see Sec. 2.1), the *Fermi*-GBM and INTEGRAL/SPI-ACS light-curves matched in time resolution and phase (see Sec. 2.2), $1.5' \times 1.5'$ postage stamps extracted from the initial six observations of SSS17a/AT 2017gfo and four early spectra taken with the SALT (at t_c+1.2 d McCully et al. 2017; Buckley et al. 2017), ESO-NTT (at t_c+1.4 d, Smartt et al. 2017), the SOAR 4-m telescope (at t_c+1.4 d, Nicholl et al. 2017), and ESO-VLT-XShooter (at t_c+2.4 d, Smartt et al. 2017) as described in Sec. 2.3, the first X-ray and radio detections of the same source by Chandra (see Sec. 3.3) and JVLA (see Sec. 3.4). In order to show representative spectral energy distributions, each spectrum is normalized to its maximum, and shifted arbitrarily along the linear y-axis (no absolute scale). The high background in the SALT spectrum below 4500 Å prevents the identification of spectral features in this band (for details McCully et al. 2017).

Evans et al. 2017), and Gemini-South (infrared, 08:00 UT; Singer et al. 2017a).

The Distance Less Than 40 Mpc survey (DLT40; L. Tartaglia et al. 2017, in prep.) team independently detected SSS17a/AT2017gfo, automatically designated DLT17ck (Yang et al. 2017a) in an image taken on Aug 17 23:50 UTC while carrying out high-priority observations of 51 galaxies (20 within in the LIGO-Virgo localization, and 31 within the wider *Fermi*-GBM localization region) (Valenti et al. 2017, accepted). A confirmation image was taken on Aug 18 00:41 UTC after the observing program had cycled through all of the high-priority targets and found no other transients. The updated magnitudes for these two epochs are r=17.18±0.03 and 17.28±0.04 mag, respectively.

SSS17a/AT2017gfo was also observed by the Visible and Infrared Survey Telescope for Astronomy (VISTA) in the second of two 1.5 square-degree fields targeted. The fields were chosen to be within the high-likelihood localization region of GW170817 and to contain a high density of potential host galaxies (32 of the 54 entries in the list of Cook et al. 2017a). Observations began during evening twilight and were repeated twice to give a short temporal baseline over which to search for variability (or proper motion of any candidates). The magnitudes of the transient source in the earliest images taken in the near-infrared, were measured to be $K_s = 18.63 \pm 0.05$, $J = 17.88 \pm 0.03$ and $Y = 17.51 \pm 0.02$ mag.

On Aug 17 23:59 UTC, the MASTER-OAFA robotic telescope (Lipunov et al. 2010), covering the sky location of GW170817, recorded an image that included NGC 4993. The auto-detection software identified MASTER OT J130948.10-232253.3, the bright optical transient with the unfiltered magnitude $W = 17.5 \pm 0.2$ mag, as part of an automated search performed by the MASTER Global Robotic Net (Lipunov et al. 2017; Lipunov et al. 2017a).

The Dark Energy Camera (DECam; Flaugher et al. 2015) Survey team started observations of the GW170817 localization region on Aug 17 23:13 UTC. DECam covered 95% of the probability in the GW170817 localization area with a sensitivity sufficient to detect a source up to 100 times fainter than the observed optical transient. The transient was observed on 2017 August 18 at 00:05 UTC and independently detected at 00:42 UTC (Allam et al. 2017). The measured magnitudes of the transient source in the first images were $i = 17.30 \pm 0.02$, $z = 17.45 \pm 0.03$. A complete analysis of DECam data is presented in Soares-Santos et al. (2017).

Las Cumbres Observatory (LCO Brown et al. 2013) surveys started their observations of individual galaxies with their global network of 1 m and 2 m telescopes upon receipt of the initial *Fermi*-GBM localization. Approximately five hours later, when the LIGO-Virgo localization map was issued, the observations were switched to a prioritized list of galaxies (from Dalya et al. 2016) ranked by distance and luminosity (Arcavi et al. 2017a). In a 300-second w-band exposure beginning on Aug 18 00:15 UTC, a new transient, corresponding to AT2017gfo/SSS17a/DLT17ck, was detected near NGC 4993 (Arcavi et al. 2017a). The transient was determined to have $w = 17.49 \pm 0.04$ mag (Arcavi et al. 2017b).

These early photometric measurements, from the optical to near-infrared, gave the first broadband spectral energy distribution of AT2017gfo/SSS17a/DL17ck. They do not distinguish the transient from a young supernova, but they serve as reference values for subsequent observations which reveal the nature of the optical counterpart as described in section 3.1. Images from the six earliest observations are shown in the inset of Figure 2.

3. BROADBAND FOLLOW-UP

While some of the first observations aimed to tile the error region of the GW170817 and GRB170817A localization areas, including the use of galaxy targeting (Dalya et al. 2016; White et al. 2011; Cook & Kasliwal 2017), most groups focused their effort on the optical transient reported by Coulter et al. (2017) to define its nature and to rule out that it was a chance coincidence of an unrelated transient. The multi-wavelength evolution within the first 12 to 24 hrs, and the subsequent discoveries of the X-ray and radio counterparts proved key to scientific interpretation. This section summarizes the plethora of key observations that occurred in different wavebands, as well as searches for neutrino counterparts.

3.1. *Ultraviolet, optical, and infrared*

The quick discovery in the first few hours of Chilean darkness, and possibility of fast evolution, prompted the need for the ultraviolet-optical-infrared follow-up community to have access to both space-based and longitudinally-separated ground-based facilities. Over the next two weeks, a network of ground-based telescopes, from 40 cm to 10 m, and space-based observatories spanning the ultraviolet (UV), optical (O) and near-infrared (IR) wavelengths followed up GW170817. These observations revealed an exceptional electromagnetic counterpart through careful monitoring of its spectral energy distribution. Here we first consider photometric and then spectroscopic observations of the source.

Regarding photometric observations, at t_c+11.6 hr, the Magellan-Clay and Magellan-Baade telescopes (Drout et al. 2017; Simon et al. 2017) initiated follow-up observations of the transient discovered by the Swope Supernova Survey from the optical (g-band) to NIR (Ks-band). At t_c+12.7 hr and t_c+12.8 hr, the Rapid Eye Mount (REM)/ROS2 (Melandri et al. 2017b) detected the optical transient and the Gemini-South FLAMINGO2 instrument first detected near-infrared Ks-band emission constraining the early optical to infrared color (Singer et al. 2017a; Kasliwal et al. 2017) respectively. At t_c+15.3 hr, the *Swift* satellite (Gehrels 2004)

detected bright, ultraviolet emission, further constraining the effective temperature (Evans et al. 2017; Evans et al. 2017). The ultraviolet evolution continued to be monitored with the *Swift* satellite (Evans et al. 2017) and the *Hubble* space telescope (Adams et al. 2017; Kasliwal et al. 2017; P. Cowperthwaite et al. 2017).

Over the course of the next two days, an extensive photometric campaign showed a rapid dimming of this initial UV-blue emission, and an unusual brightening of the near-infrared emission. After roughly a week, the redder optical and near-infrared bands began to fade as well. Ground-based facilities participating in this photometric monitoring effort include (in alphabetic order): CTIO1.3m, DECam (Nicholl et al. 2017a; P. Cowperthwaite et al. 2017; Nicholl et al. 2017), IRSF, the Gemini-South FLAMINGO2 (Singer et al. 2017a; Troja et al. 2017a; Chornock et al. 2017a; Troja et al. 2017b; Singer et al. 2017b), Gemini-South GMOS (Troja et al. 2017a), GROND (Wiseman et al. 2017; Chen et al. 2017), Hubble Space Telescope (HST Levan et al. 2017a; Tanvir & Levan 2017; Troja et al. 2017; Levan & Tanvir 2017; P. Cowperthwaite et al. 2017), iTelescope.Net telescopes (Im et al. 2017a,b), the Korea Microlensing Telescope Network (KMTNet Im et al. 2017c,d), Las Cumbres Observatory (Arcavi et al. 2017b; Arcavi et al. 2017b,c), the Lee Sang Gak Telescope (LSGT)/SNUCAM-II, the Magellan-Baade and Magellan-Clay 6.5-m telescopes (Simon et al. 2017; Drout et al. 2017), the Nordic Optical Telescope (Malesani et al. 2017a), Pan-STARRS1 (Chambers et al. 2017a,b,c,d), REM/ROS2 and REM/REMIR (Melandri et al. 2017a,c), SkyMapper (Wolf et al. 2017), Subaru Hyper Suprime-Cam (Yoshida et al. 2017a,b,c,d; Tominaga et al. 2017), ESO-VISTA (Tanvir et al. 2017a), ESO-VST/OmegaCAM (Grado et al. 2017a,b), and ESO-VLT/FORS2 (D'Avanzo et al. 2017).

One of the key properties of the transient that alerted the world-wide community to its unusual nature was the rapid luminosity decline. In bluer optical bands (i.e., in the g-band) the transient showed a fast decay between daily photometric measurements (Melandri et al. 2017c; P. Cowperthwaite et al. 2017). Pan-STARRS (Chambers et al. 2017c) reported photometric measurements in the optical/infrared izy-bands with the same cadence, showing fading by 0.6 mag per day, with reliable photometry from difference imaging using already existing sky images (Chambers et al. 2016; P. Cowperthwaite et al. 2017). Observations taken every 8 hours by Las Cumbres Observatory showed an initial rise in the w-band, followed by rapid fading in all optical bands (more than 1 mag per day in the blue), and reddening with time (Arcavi et al. 2017b). Accurate measurements from Subaru (Tominaga et al. 2017), LSGT/SNUCAM-II and KMTNet (Im et al. 2017c), ESO-VLT/FORS2 (D'Avanzo et al. 2017), and DECam (Nicholl et al. 2017b; P. Cowperthwaite et al. 2017) indicated a similar rate of fading. On the contrary, the near-infrared monitoring reports by GROND and Gemini-South, showed that the source faded more slowly in the infrared (Wiseman et al. 2017; Chornock et al. 2017a) and even showed a late-time plateau in Ks-band (Singer et al. 2017b). This evolution was recognized by the community as quite unprecedented for transients in the nearby (within 100 Mpc) Universe (e.g., Siebert et al. 2017).

Table 1 reports a summary of the imaging observations, which include coverage of the entire gravitational-wave sky localization and follow-up of SSS17a/AT 2017gfo . Figure 2 shows these observations in graphical form.

Concerning spectroscopic observations, immediately after discovery of SSS17a/AT2017gfo on the Swope 1 m telescope, the same team obtained the first spectroscopic observations of the optical transient with the LDSS-3 spectrograph on the 6.5m Magellan-Clay telescope and the MagE spectrograph on the 6.5m Magellan-Baade telescope at Las Campanas Observatory. The spectra, just 30 minutes after the first image showed a blue and featureless continuum between 4,000 AA and 10,000 AA, consistent with a power-law (Drout et al. 2017; Shappee et al. 2017). The lack of features and blue continuum during the first few hours implied an unusual, but not unprecedented transient since such characteristics are common in cataclysmic-variable stars and young core-collapse supernovae (see e.g., Li et al. 2011b,a).

The next 24 hours of observation were critical in decreasing the likelihood of a chance coincidence between SSS17a/AT 2017gfo , GW170817, and GRB170817A. The SALT-RSS spectrograph in South Africa (Shara et al. 2017; McCully et al. 2017; Buckley et al. 2017), the ePESSTO with the EFOSC2 instrument in spectroscopic mode at the ESO New Technology Telescope (NTT, in La Silla, Chile; Lyman et al. 2017), the X-shooter spectrograph on the ESO Very Large Telescope (Pian et al. 2017) in Paranal, the Goodman Spectrograph on the 4m SOAR telescope (Nicholl et al. 2017c) obtained additional spectra. These groups reported a rapid fall-off in the blue spectrum without any individual features identifiable with line absorption common in supernova-like transients (see e.g., Lyman et al. 2017). This ruled out a young supernova of any type in NGC 4993, showing an exceptionally fast spectral evolution (Drout et al. 2017; Nicholl et al. 2017). Figure 2 shows some representative early spectra (SALT spectrum is from McCully et al. 2017; Buckley et al. 2017, ESO spectra from Smartt et al. 2017 and SOAR spectrum from (Nicholl et al. 2017)). These show rapid cooling, and the lack of commonly observed ions from elements abundant in supernova ejecta, indicating this object was unprecedented in its optical and near-infrared. Combined with the rapid fading, this was broadly indicative of a possible kilonova (e.g., Kasen et al. 2017; Kasliwal et al. 2017; Smartt et al. 2017; McCully et al. 2017; Arcavi et al.

2017b; P. Cowperthwaite et al. 2017; Nicholl et al. 2017). This was confirmed by spectra taken at later times, such as with the Gemini Multi-Object Spectrograph (GMOS; Troja et al. 2017a; Troja et al. 2017; Kasliwal et al. 2017; McCully et al. 2017), the LDSS-3 spectrograph on the 6.5m Magellan-Clay telescope at Las Campanas Observatory (Drout et al. 2017; Shappee et al. 2017), the Las Cumbres Observatory FLOYDS spectrograph at Faulkes Telescope South (McCully et al. 2017; McCully et al. 2017) and the AAOmega spectrograph on the 3.9m Anglo-Australian Telescope (Andreoni et al. 2017), which did not show any significant emission or absorption lines over the red featureless continuum. The optical and near-infrared spectra over these few days provided convincing arguments that this transient was unlike any other discovered in extensive optical wide-field surveys over the last decade (see e.g., Siebert et al. 2017).

The evolution of the spectral energy distribution, rapid fading and emergence of broad spectral features indicated that the source had physical properties similar to models of kilonovae (e.g., Metzger et al. 2010; Kasen et al. 2013; Barnes & Kasen 2013; Tanaka & Hotokezaka 2013; Met ????; Grossman et al. 2014; Barnes et al. 2016; Tanaka 2016; Metzger 2017; Kasen et al. 2017). These show a very rapid shift of the spectral energy distribution from the optical to the near-infrared. The FLAMINGOS2 near-infrared spectrograph at Gemini-South (Chornock et al. 2017b; Kasliwal et al. 2017) shows the emergence of very broad features in qualitative agreement with kilonova models . The ESO-VLT/X-shooter spectra, which simultaneously cover the wavelength range 3200–24800 Å, were taken over 2 weeks with a close to daily sampling (Pian et al. 2017; Smartt et al. 2017) and revealed signatures of the radioactive decay of r-process nucleosynthesis elements (Pian et al. 2017). Three epochs of infrared grism spectroscopy with the Hubble Space Telescope (Levan et al. 2017a; Tanvir & Levan 2017; Troja et al. 2017; Levan & Tanvir 2017; P. Cowperthwaite et al. 2017)[6] identified features consistent with the production of lanthanides within the ejecta (Levan & Tanvir 2017; Tanvir & Levan 2017; Troja et al. 2017).

The optical follow-up campaign also includes linear polarimetry measurements of SSS17a/AT 2017gfo by ESO-VLT/FORS2, showing no evidence of an asymmetric geometry of the emitting region and lanthanide-rich late kilonova emission (Covino et al. 2017). In addition, the study of the galaxy with the MUSE Integral Field Spectrograph on the ESO-VLT (Levan et al. 2017b) provides simultaneous spectra of the counterpart and the host galaxy, which show broad absorption features in the transient spectrum, combined with emission lines from the spiral arms of the host galaxy (Levan & Tanvir 2017; Tanvir & Levan 2017).

Table 2 reports the spectroscopic observations, that have led to the conclusion that the source broadly matches kilonovae theoretical predictions.

[6] HST Program GO 14804 Levan, GO 14771 Tanvir & GO 14850 Troja

3.2. *Gamma-rays*

The fleet of ground- and space-based gamma-ray observatories provided broad temporal and spectral coverage of the source location. Observations spanned $\sim$10 orders of magnitude in energy and covered the position of SSS17a/AT 2017gfo from a few hundred seconds before the GRB170817A trigger time (T0) to days afterwards. Table 3 lists, in chronological order, the results reporting observation time, flux upper limits, and the energy range of the observations, which are summarized here.

At the time of GRB170817A, three out of six spacecraft of the Inter Planetary Network (Hurley et al. 2013) had a favorable orientation to observe the LIGO-Virgo sky-map. However, based on the *Fermi*-GBM (Goldstein et al. 2017) and INTEGRAL analyses, GRB170817A was too weak to be detected by Konus-*Wind* (Svinkin et al. 2017a). Using the Earth Occultation technique (Wilson-Hodge et al. 2012), *Fermi*-GBM placed limits on persistent emission for the 48-hour period centered at the *Fermi*-GBM trigger time over the 90% credible region of the GW170817 localization. Using the offline targeted search for transient signals (Blackburn et al. 2015), *Fermi*-GBM also set constraining upper limits on precursor and extended emission associated with GRB170817A (Goldstein et al. 2017). INTEGRAL (Winkler et al. 2003) continued uninterrupted observations after GRB170817A for 10 hours. Using the PiCSIT (Labanti et al. 2003) and SPI-ACS detectors, the presence of a steady source ten times weaker than the prompt emission was excluded (Savchenko et al. 2017).

The High Energy telescope on-board *Insight*-HXMT monitored the entire GW170817 sky map from $\mathrm{T0}-650$ s to $\mathrm{T0}+450$ s but, due to the weak and soft nature of GRB170817A, did not detect any significant excess at T0 (Liao et al. 2017). Upper limits from $0.2-5$ MeV for GRB170817A and other emission episodes are reported in Li et al. (2017).

The Calorimetric Electron Telescope (CALET) Gamma-ray Burst Monitor (CGBM) found no significant excess around T0. Upper limits may be affected due to the location of SSS17a/AT 2017gfo being covered by the large structure of the International Space Station at the time of GRB170817A (Nakahira et al. 2017). *AstroSat* CZTI (Singh et al. 2014; Bhalerao et al. 2017) reported upper limits for the 100 s interval centered on T0 (Balasubramanian et al. 2017); the position of SSS17a/AT 2017gfo was occulted by the Earth, however, at the time of the trigger.

For the AstroRivelatore Gamma a Immagini Leggero (AGILE) satellite (Tavani et al. 2009) the first exposure of the GW170817 localization region by the Gamma Ray Imaging Detector (GRID), which was occulted by the Earth at the time of GRB170817A started at $T0 + 935$ s. The GRID observed the field before and after T0, typically with 150 s exposures. No gamma-ray source was detected above 3σ in the energy range 30 MeV–30 GeV (Verrecchia et al. 2017).

At the time of the trigger, *Fermi* was entering the South Atlantic Anomaly (SAA) and the Large Area Telescope (LAT) was not collecting science data (*Fermi*-GBM uses different SAA boundaries and was still observing). *Fermi*-LAT resumed data taking at roughly $T0 + 1153$ s, when 100% of the low-latency GW170817 sky-map (The LIGO Scientific Collaboration et al. 2017b) was in the field of view for $\sim$1000 s. No significant source of high-energy emission was detected. Additional searches over different time scales were performed for the entire time span of LAT data, and no significant excess was detected at the position of SSS17a/AT 2017gfo (Kocevski et al. 2017).

The High Energy Stereoscopic System (H.E.S.S.) array of imaging atmospheric Cherenkov telescopes observed from August 17 18:00 UTC with three pointing positions. The first, at $T0 + 5.3$ hr, covered SSS17a/AT 2017gfo. Observations repeated the following nights until the location moved outside the visibility window, with the last pointing performed on August 22 18:15 UTC. A preliminary analysis with an energy threshold of $\sim$500 GeV revealed no significant gamma-ray emission (de Naurois et al. 2017), confirmed by the final, offline analysis (see Abdalla, H. et al. (H.E.S.S. Collaboration) (2017) for more results).

For the High-Altitude Water Cherenkov (HAWC) Observatory (Abeysekara et al. 2017) the LIGO-Virgo localization region first became visible on August 17 between 19:57 and 23:25 UTC. SSS17a/AT 2017gfo was observed for 2.03 hours starting at 20:53 UTC. Upper limits from HAWC for energies > 40 TeV assuming an $E^{-2.5}$ spectrum are reported in Martinez-Castellanos et al. (2017).

INTEGRAL (3 keV–8 MeV) carried out follow-up observations of the LIGO-Virgo localization region, centered on the optical counterpart, starting 24 hours after the event and spanning 4.7 days. Hard X-ray emission is mostly constrained by IBIS (Ubertini et al. 2003), while above 500 keV SPI (Vedrenne et al. 2003) is more sensitive. Besides the steady flux limits reported in Table 3, these observations exclude delayed bursting activity at the level of giant magnetar flares. No gamma-ray lines from a kilonova or $e^{+/-}$ pair plasma annihilation were detected (see Savchenko et al. 2017).

3.3. *Discovery of the X-ray counterpart*

While the UV, optical, and IR observations mapped the emission from the sub-relativistic ejecta, X-ray observations probed a different physical regime. X-ray observations of GRB afterglows are important to constrain the geometry of the outflow, its energy output, and the orientation of the system with respect to the observers' line of sight.

The earliest limits at X-ray wavelengths were provided by the Gas Slit Camera (GSC) of the Monitor of All-Sky X-ray Image (MAXI; Matsuoka et al. 2009). Due to an unfavorable sky position, the location of GW 170817 was not observed by MAXI until August 17 17:21 UTC ($T0 + 0.19$ d). No X-ray emission was detected at this time to a limiting flux of 8.6×10^{-9} erg cm^{-2} s^{-1} (2–10 keV; Sugita et al. 2017; Sugita et al. in prep.). MAXI obtained three more scans over the location with no detections before the more sensitive pointed observations began.

In addition, the Super-*AGILE* detector (Feroci et al. 2007) onboard the *AGILE* mission (Tavani et al. 2009) observed the location of GW170817 starting at August 18 01:16:34.84 UTC ($T0 + 0.53$ d). No X-ray source was detected at the location of GW170817, with a 3σ upper limit of 3.0×10^{-9} erg cm^{-2} s^{-1} ($18 - 60$ keV) (Verrecchia et al. 2017).

The first pointed X-ray observations of GW170817 were obtained by the X-Ray Telescope (Burrows et al. 2005) on the *Swift* satellite (Gehrels 2004) and the NUclear Spectroscopic Telescope ARray (*NuSTAR*; Harrison et al. 2013), beginning at $T0 + 0.62$ d and $T0 + 0.70$ d, respectively. No X-ray emission was detected at the location of GW170817 to limiting fluxes of 2.7×10^{-13} erg cm^{-2} s^{-1} ($0.3 - 10.0$ keV; Evans et al. 2017; Evans et al. 2017) and 2.6×10^{-14} erg cm^{-2} s^{-1} ($3.0 - 10.0$ keV; Evans et al. 2017; Evans et al. 2017). *Swift* continued to monitor the field, and after stacking several epochs of observations, a weak X-ray source was detected near the location of GW170817 at a flux of 2.6×10^{-14} erg cm^{-2} s^{-1} (Evans et al. 2017).

INTEGRAL (see Section 3.2) performed pointed follow-up observations from one to about six days after the trigger. The X-ray monitor JEM-X (Lund et al. 2003) constrained the average X-ray luminosity at the location of the optical transient to be $< 2 \times 10^{-11}$ erg cm^{-2} s^{-1} ($3 - 10.0$ keV) and $< 7 \times 10^{-12}$ erg cm^{-2} s^{-1} ($10 - 25$ keV; Savchenko et al. 2017).

Chandra obtained a series of observations of GW170817 beginning at August 19 17:10 UTC ($T0 + 2.2$ d) and continuing until the emission from NGC 4993 became unobservable because SSS17a/AT 2017gfo's proximity to the Sun (Margutti et al. 2017; Troja et al. 2017a; Fong et al. 2017; Troja et al. 2017b; Haggard et al. 2017b). Two days post-trigger, Margutti et al. (2017) reported an X-ray non-detection for SSS17a/AT 2017gfo in a $\simeq$25 ks *Chan-*

dra exposure[7], along with the detection of an extended X-ray source whose position was consistent with the host NGC 4993 (R. Margutti et al. 2017). Refined astrometry from subsequent Swift observations confirmed that the previously reported candidate was indeed associated with the host nucleus (Evans et al. 2017; Evans et al. 2017).

Nine days post-trigger, Troja et al. (2017a) reported the discovery of the X-ray counterpart with *Chandra*. In a 50 ks exposure observation they detected significant X-ray emission at the same position of the optical/IR counterpart (Troja et al. 2017, top right panel in Figure 2)[8]. Fifteen days post-trigger, two additional 50 ks *Chandra* observations were made, which confirmed the continued presence of X-ray emission. Based on the first of these two observations[9],[10]: Fong et al. (2017) reported the detection of the X-ray counterpart and the presence of an additional X-ray point source in the near vicinity (R. Margutti et al. 2017), and Troja et al. (2017b) reported a flux of 4.5×10^{-15} erg cm^{-2} s^{-1} for the X-ray counterpart. One day later, Haggard et al. (2017b) reported another deep observation showing continued distinct X-ray emission coincident with SSS17a/AT 2017gfo, NGC 4993, and the additional point source (Haggard et al. 2017b,a).[10]

Neither *Swift* nor *Chandra* can currently observe GW170817 because it is too close to the Sun ($< 47^\circ$ for *Swift*, $< 46^\circ$ for *Chandra*). Hence, until early December 2017, *NuSTAR* is the only sensitive X-ray observatory that can continue to observe the location of GW170817.

All X-ray observations of GW170817 are summarized in Table 4.

3.4. *Discovery of the Radio Counterpart*

Radio emission traces fast-moving ejecta from a neutron star coalescence, providing information on the energetics of the explosion, the geometry of the ejecta, as well as the environment of the merger. The spectral and temporal evolution of such emission, coupled with X-ray observations, are likely to constrain several proposed models (see e.g., Nakar & Piran 2011; Piran et al. 2013; Hotokezaka & Piran 2015; Hotokezaka et al. 2016; Gottlieb et al. 2017).

Prior to detection of SSS17a/AT2017gfo, a blind radio survey of cataloged galaxies in the gravitational-wave localization volume commenced with the Australian Telescope Compact Array (ATCA, Wilson et al. 2011), and observed the merger events location on August 18, 2017 at 01:46 UTC (Kaplan et al. 2017a). In addition, the Long Wavelength Array 1 (LWA1, Ellingson et al. 2013) followed up the gravitational-wave localization 6.5 hr after the time of coalescence (Callister et al. 2017a). A preliminary analysis suggested the possible presence of a variable radio source (Callister et al. 2017b). Analysis of follow-up observations, however, proved inconclusive. Further study of the LWA1 data is ongoing, including the exploration of flux density upper limits at 25 and 45 MHz.

The first reported radio observations of the optical transient SSS17a/AT 2017gfo 's location occurred on Aug 18 at 02:09:00 UTC (T0+13.5 hr) with the Karl G. Jansky Very Large Array (VLA) by Alexander et al. (2017a).[11] Initially attributed to the optical transient, this radio source was later established to be an AGN in the nucleus of the host galaxy, NGC 4993 (Alexander et al. 2017b; K. Alexander et al. 2017). Subsequent observations with several radio facilities spanning a wide range of radio and millimeter frequencies continued to detect the AGN, but did not reveal radio emission at the position of the transient (Bannister et al. 2017a; Kaplan et al. 2017a; De et al. 2017a; Alexander et al. 2017c; Corsi et al. 2017a,b; De et al. 2017b; Mooley et al. 2017a; Lynch et al. 2017a; Corsi et al. 2017c; Lynch et al. 2017b,c; Resmi et al. 2017).

The first radio counterpart detection consistent with the HST position (refined by Gaia astrometry) of SSS17a/AT 2017gfo (Adams et al. 2017) was obtained with the VLA on September 2 and 3, 2017 at two different frequencies ($\approx$ 3 GHz and $\approx$ 6 GHz) via two independent observations: the Jansky VLA mapping of Gravitational Wave bursts as Afterglows in Radio (JAGWAR) [12] (Mooley et al. 2017b) and VLA/16A-206[13] (Corsi et al. 2017d). Marginal evidence for radio excess emission at the location of SSS17a/AT 2017gfo was also confirmed in ATCA images taken on September 5 at similar radio frequencies ($\approx$ 7.25 GHz; Murphy et al. 2017). Subsequent repeated detections spanning multiple frequencies have confirmed an evolving transient (Hallinan et al. 2017,Hallinan, Corsi et al. 2017, Corsi et al., 2017, Mooley et al. 2017). Independent observations carried out on September 5, 2017 with the same frequency and exposure time used by Corsi et al. (2017d) did not detect any emission to a 5-σ limit[14] (Alexander et al. 2017d), but this group also subsequently detected the radio counterpart on September 25 2017 (Alexander et al. 2017e; K. Alexander et al. 2017).

SSS17a/AT 2017gfo, as well as other parts of the initial gravitational-wave localization area, were and are also being continuously monitored at a multitude of different frequencies with the Atacama Large Millimeter Array

[7] *Chandra* OBSID-18955, PI: Fong
[8] Chandra OBSID-19294, PI:Troja
[9] Chandra OBSID-20728, PI: Troja (Director's Discretionary Time observation distributed also to Haggard, Fong, and Margutti)
[10] Chandra OBSID-18988, PI: Haggard
[11] VLA/17A-218, PI: Fong
[12] VLA/17A-374, PI: Mooley
[13] VLA/16A-206, PI: Corsi
[14] VLA/17A-231, PI: Alexander

(ALMA; Wootten & Thompson 2009; Schulze et al. 2017; Kim et al. 2017; K. Alexander et al. 2017; Williams et al. 2017a), the Australian Square Kilometre Array Pathfinder (ASKAP; Johnston et al. 2007), ASKAP-Fast Radio Burst (Bannister et al. 2017b; Bannister et al. 2017), ATCA, Effelsberg-100 m (Barr et al. 2013), the Giant Metrewave Radio Telescope (GMRT; Swarup et al. 1991), the Low Frequency Array (LOFAR; van Haarlem et al. 2013), the Long Wavelength Array (LWA1), MeerKAT (Goedhart et al. 2017a), the Murchison Widefield Array (MWA; Tingay et al. 2013), Parkes-64 m (SUPERB, Bailes et al. 2017a, Keane et al. 2017), Sardinia Radio Telescope (SRT; Prandoni et al. 2017), VLA, VLA Low Band Ionosphere and Transient Experiment (VLITE; Clarke et al. 2016), and also using the very long baseline interferometry (VLBI) technique with e-MERLIN (Moldon et al. 2017a,b), the European VLBI Network (Paragi et al. 2017a,b), and the Very Long Baseline Array (VLBA; Deller et al. 2017a,b). The latter have the potential to resolve (mildly) relativistic ejecta on a timescale of months.

Table 5 summarizes the radio observations of GW170817.

3.5. *Neutrinos*

The detection of GW170817 was rapidly followed up by the IceCube (Aartsen et al. 2017) and ANTARES (Ageron et al. 2011) neutrino observatories and the Pierre Auger Observatory (Aab et al. 2015a) to search for coincident, high-energy (GeV-EeV) neutrinos emitted in the relativistic outflow produced by the BNS merger. The results from these observations, described briefly below, can be used to constrain the properties of relativistic outflows driven by the merger (Albert, A., et al. 2017, in prep.).

In a search for muon-neutrino track candidates (Aartsen et al. 2016), and contained neutrino events of any flavor (Aartsen et al. 2015), IceCube identified no neutrinos that were directionally coincident with the final localization of GW170817 at 90% credible level, within ± 500 s of the merger (Bartos et al. 2017a,b). Additionally, no MeV supernova neutrino burst signal was detected coincident with the merger. Following the identification via electromagnetic observations of the host galaxy of the event, IceCube also carried out an extended search in the direction of NGC 4993 for neutrinos within the 14-day period following the merger, but found no significant neutrino emission (Albert, A., et al. 2017, in prep.).

A neutrino search for up-going high-energy muon neutrinos was carried out using the online ANTARES data stream (Ageron et al. 2017a). No up-going neutrino candidates were found over a $t_c \pm 500$ s time window. The final localization of GW170817 (The LIGO Scientific Collaboration et al. 2017c) was above the ANTARES horizon at the time of the GW event. A search for down-going muon neutrinos was thus performed and no neutrinos were found over $t_c \pm 500$ s (Ageron et al. 2017b). A search for neutrinos originating from below the ANTARES horizon, over an extended period of 14 days after the merger, was also performed, without yielding significant detection (Albert, A., et al. 2017, in prep.).

The Pierre Auger Observatory carried out a search for ultra high-energy (UHE) neutrinos above $\sim 10^{17}$ eV using its Surface Detector (Aab et al. 2015a). UHE neutrino-induced extensive air showers produced either by interactions of downward-going neutrinos in the atmosphere or by decays of tau leptons originating from tau neutrino interactions in the Earth's crust can be efficiently identified above the background of the more numerous ultra-high energy cosmic rays (Aab et al. 2015b). Remarkably, the position of the transient in NGC 4993 was just between 0.3 and 3.2 degrees below the horizon during $t_c \pm 500$ s. This region corresponds to the most efficient geometry for Earth-skimming tau neutrino detection at 10^{18} eV energies. No neutrino candidates were found in $t_c \pm 500$ s (Alvarez-Muniz et al. 2017) nor in a 14-day period after it (Albert, A., et al. 2017, in prep.).

4. CONCLUSION

For the first time, gravitational and electromagnetic waves from a single source have been observed. The gravitational wave observation of a binary neutron star merger is the first of its kind. The electromagnetic observations further support the interpretation of the nature of the binary, and comprise three components at different wavelengths: (i) a prompt, sGRB which demonstrates that BNS mergers are the central engine of at least a fraction of such bursts; (ii) an ultraviolet, optical and infrared transient (kilonova), which allows for the identification of the host galaxy and is associated with the aftermath of the BNS merger; and (iii) delayed X-ray and radio counterparts which provide information on the environment of the binary. These observations, described in detail in the companion articles cited above, offer a comprehensive, sequential description of the physical processes related to the merger of a binary neutron star. The results of this campaign demonstrate the importance of collaborative gravitational-wave, electromagnetic and neutrino observations, and mark a new era in multi-messenger, time-domain astronomy.

APPENDIX

A. SUPPLEMENTARY INFORMATION

Table 1. A partial summary of photometric observations up to Sep 5 2017 UTC with at most 3 observations per filter per telescope/group, i.e. the earliest, the peak, and the latest in each case. This is a subset of all the observations made in order to give a sense of the substantial coverage of this event.

Telescope/Instrument	UT date	Band	References
DFN/–	2017-08-17 12:41:04	visible	Hancock et al. (2017),
MASTER/–	2017-08-17 17:06:47	Clear	V.M.Lipunov et al. (2017a), Lipunov et al. (2017)
PioftheSky/PioftheSkyNorth	2017-08-17 21:46:28	visible wide band	Cwiek et al. (2017), Batsch et al. (2017), Zadrożny et al. (2017)
MASTER/–	2017-08-17 22:54:18	Visible	V.M.Lipunov et al. (2017a), Lipunov et al. (2017)
Swope/DirectCCD	2017-08-17 23:33:17	i	Coulter et al. (2017a), Coulter et al. (2017b), Coulter et al. (2017)
PROMPT5(DLT40)/–	2017-08-17 23:49:00	r	Yang et al. (2017a), Valenti et al (submitted)
VISTA/VIRCAM	2017-08-17 23:55:00	K	Tanvir & Levan (2017)
MASTER/–	2017-08-17 23:59:54	Clear	Lipunov et al. (2017a), Lipunov et al. (2017)
Blanco/DECam/–	2017-08-18 00:04:24	i	P. Cowperthwaite et al. (2017)
Blanco/DECam/–	2017-08-18 00:05:23	z	P. Cowperthwaite et al. (2017)
VISTA/VIRCAM	2017-08-18 00:07:00	J	Tanvir & Levan (2017)
Magellan-Clay/LDSS3-C	2017-08-18 00:08:13	g	Simon et al. (2017), Drout et al. (2017)
Magellan-Baade/FourStar	2017-08-18 00:12:19	H	Drout et al. (2017)
LasCumbres1-m/Sinistro	2017-08-18 00:15:50	w	Arcavi et al. (2017a), Arcavi et al. (2017b)
VISTA/VIRCAM	2017-08-18 00:17:00	Y	Tanvir & Levan (2017)
MASTER/–	2017-08-18 00:19:05	Clear	Lipunov et al. (2017a), Lipunov et al. (2017)
Magellan-Baade/FourStar	2017-08-18 00:25:51	J	Drout et al. (2017)
Magellan-Baade/FourStar	2017-08-18 00:35:19	Ks	Drout et al. (2017)
PROMPT5(DLT40)/–	2017-08-18 00:40:00	r	Yang et al. (2017a), Valenti et al (submitted)
REM/ROS2	2017-08-18 01:24:56	g	Melandri et al. (2017a), Pian et al. (2017)
REM/ROS2	2017-08-18 01:24:56	i	Melandri et al. (2017a), Pian et al. (2017)
REM/ROS2	2017-08-18 01:24:56	z	Melandri et al. (2017a), Pian et al. (2017)
REM/ROS2	2017-08-18 01:24:56	r	Melandri et al. (2017a), Pian et al. (2017)
Gemini-South/Flamingos-2	2017-08-18 01:30:00	Ks	Singer et al. (2017a), Kasliwal et al. (2017)
PioftheSky/PioftheSkyNorth	2017-08-18 03:01:39	visible wide band	Cwiek et al. (2017), Batsch et al. (2017),
Swift/UVOT	2017-08-18 03:37:00	uvm2	Evans et al. (2017), Evans et al. (2017)
Swift/UVOT	2017-08-18 03:50:00	uvw1	Evans et al. (2017), Evans et al. (2017)
Swift/UVOT	2017-08-18 03:58:00	u	Evans et al. (2017), Evans et al. (2017)
Swift/UVOT	2017-08-18 04:02:00	uvw2	Evans et al. (2017), Evans et al. (2017)
Subaru/HyperSuprime-Cam	2017-08-18 05:31:00	z	Yoshida et al. (2017a), Yoshida et al. (2017b), Utsumi, Y., et al. (i
Pan-STARRS1/–	2017-08-18 05:33:00	y	Chambers et al. (2017a), Smartt et al. (2017)
Pan-STARRS1/–	2017-08-18 05:34:00	z	Chambers et al. (2017a), Smartt et al. (2017)
Pan-STARRS1/–	2017-08-18 05:35:00	i	Chambers et al. (2017a), Smartt et al. (2017)
Pan-STARRS1/–	2017-08-18 05:36:00	y	Chambers et al. (2017a), Smartt et al. (2017)
Pan-STARRS1/–	2017-08-18 05:37:00	z	Chambers et al. (2017a), Smartt et al. (2017)
Pan-STARRS1/–	2017-08-18 05:38:00	i	Chambers et al. (2017a), Smartt et al. (2017)
LasCumbres1-m/Sinistro	2017-08-18 09:10:04	w	Arcavi et al. (2017b), Arcavi et al. (2017b)
SkyMapper/–	2017-08-18 09:14:00	i	–
SkyMapper/–	2017-08-18 09:35:00	z	–
LasCumbres1-m/Sinistro	2017-08-18 09:37:26	g	Arcavi et al. (2017b)

Table 1 continued

Table 1 *(continued)*

Telescope/Instrument	UT date	Band	References
SkyMapper/–	2017-08-18 09:39:00	r	–
SkyMapper/–	2017-08-18 09:41:00	g	–
LasCumbres1-m/Sinistro	2017-08-18 09:43:11	r	Arcavi et al. (2017b)
T17/–	2017-08-18 09:47:13	g	Im et al. (2017a), Im et al. (2017b), Im et al. (in prepara
SkyMapper/–	2017-08-18 09:50:00	v	–
T17/–	2017-08-18 09:56:46	r	Im et al. (2017a), Im et al. (2017b), Im et al. (in prepara
SkyMapper/–	2017-08-18 10:01:00	i	Wolf et al. (2017),
SkyMapper/–	2017-08-18 10:03:00	r	Wolf et al. (2017),
SkyMapper/–	2017-08-18 10:05:00	g	Wolf et al. (2017),
T17/–	2017-08-18 10:06:18	i	Im et al. (2017a), Im et al. (2017b), Im et al. (in prepara
SkyMapper/–	2017-08-18 10:07:00	v	Wolf et al. (2017),
LSGT/SNUCAM-II	2017-08-18 10:08:01	m425	Im et al. (2017a), Im et al. (2017b), Im et al. (in prepara
SkyMapper/–	2017-08-18 10:09:00	u	Wolf et al. (2017),
LSGT/SNUCAM-II	2017-08-18 10:12:48	m475	Im et al. (2017a), Im et al. (2017b), Im et al. (in prepara
LSGT/SNUCAM-II	2017-08-18 10:15:16	m525	Im et al. (2017a), Im et al. (2017b), Im et al. (in prepara
T17/–	2017-08-18 10:15:49	z	Im et al. (2017a), Im et al. (2017b), Im et al. (in prepara
LSGT/SNUCAM-II	2017-08-18 10:21:14	m575	Im et al. (2017a), Im et al. (2017b), Im et al. (in prepara
LSGT/SNUCAM-II	2017-08-18 10:22:33	m625	Im et al. (2017a), Im et al. (2017b), Im et al. (in prepara
AST3-2/wide-fieldcamera	2017-08-18 13:11:49	g	Hu et al. (2017),
Swift/UVOT	2017-08-18 13:30:00	uvm2	Cenko et al. (2017), Evans et al. (2017)
Swift/UVOT	2017-08-18 13:37:00	uvw1	Cenko et al. (2017), Evans et al. (2017)
Swift/UVOT	2017-08-18 13:41:00	u	Cenko et al. (2017), Evans et al. (2017)
IRSF/SIRIUS	2017-08-18 16:34:00	Ks	Utsumi, Y., et al. (in press)
IRSF/SIRIUS	2017-08-18 16:34:00	H	Utsumi, Y., et al. (in press)
IRSF/SIRIUS	2017-08-18 16:48:00	J	Utsumi, Y., et al. (in press)
KMTNet-SAAO/wide-fieldcamera	2017-08-18 17:00:36	B	Im et al. (2017d), Im et al. (2017c), Troja et al. (2017)
KMTNet-SAAO/wide-fieldcamera	2017-08-18 17:02:55	V	Im et al. (2017d), Im et al. (2017c), Troja et al. (2017)
KMTNet-SAAO/wide-fieldcamera	2017-08-18 17:04:54	R	Im et al. (2017d), Im et al. (2017c), Troja et al. (2017)
MASTER/–	2017-08-18 17:06:55	Clear	Lipunov et al. (2017b), Lipunov et al. (2017)
KMTNet-SAAO/wide-fieldcamera	2017-08-18 17:07:12	I	Im et al. (2017d), Im et al. (2017c), Troja et al. (2017)
MASTER/–	2017-08-18 17:17:33	R	V.M.Lipunov et al. (2017b), V.M.Lipunov et al. (2017a), Lipunov et al. (2017)
MASTER/–	2017-08-18 17:34:02	B	V.M.Lipunov et al. (2017a), Lipunov et al. (2017)
1.5B/–	2017-08-18 18:12:00	r	Smartt et al. (2017)
MPG2.2m/GROND/–	2017-08-18 18:12:00	g	Smartt et al. (2017)
NOT/NOTCam	2017-08-18 20:24:08	Ks	Malesani et al. (2017a), Tanvir & Levan (2017)
NOT/NOTCam	2017-08-18 20:37:46	J	Malesani et al. (2017a), Tanvir & Levan (2017)
PioftheSky/PioftheSkyNorth	2017-08-18 21:44:44	visible wide band	Cwiek et al. (2017), Batsch et al. (2017),
LasCumbres1-m/Sinistro	2017-08-18 23:19:40	i	Arcavi et al. (2017b)
Blanco/DECam/–	2017-08-18 23:25:56	Y	P. Cowperthwaite et al. (2017)
Magellan-Clay/LDSS3-C	2017-08-18 23:26:33	z	Drout et al. (2017)
Blanco/DECam/–	2017-08-18 23:26:55	z	P. Cowperthwaite et al. (2017)
Blanco/DECam/–	2017-08-18 23:27:54	i	P. Cowperthwaite et al. (2017)
KMTNet-CTIO/wide-fieldcamera	2017-08-18 23:28:35	B	Im et al. (2017d), Im et al. (2017c), Troja et al. (2017)
Blanco/DECam/–	2017-08-18 23:28:53	r	P. Cowperthwaite et al. (2017)
Blanco/DECam/–	2017-08-18 23:29:52	g	P. Cowperthwaite et al. (2017)
KMTNet-CTIO/wide-fieldcamera	2017-08-18 23:30:31	V	Im et al. (2017d), Im et al. (2017c), Troja et al. (2017)
Blanco/DECam/–	2017-08-18 23:30:50	u	P. Cowperthwaite et al. (2017)
Magellan-Clay/LDSS3-C	2017-08-18 23:30:55	i	Drout et al. (2017)
REM/ROS2	2017-08-18 23:31:02	z	Melandri et al. (2017c), Pian et al. (2017)

Table 1 continued

Table 1 *(continued)*

Telescope/Instrument	UT date	Band	References
Magellan-Clay/LDSS3-C	2017-08-18 23:32:02	r	Drout et al. (2017)
KMTNet-CTIO/wide-fieldcamera	2017-08-18 23:32:36	R	Im et al. (2017d), Im et al. (2017c), Troja et al. (2017)
Magellan-Baade/FourStar	2017-08-18 23:32:58	J	Drout et al. (2017)
KMTNet-CTIO/wide-fieldcamera	2017-08-18 23:34:48	I	Im et al. (2017d), Im et al. (2017c), Troja et al. (2017)
Magellan-Clay/LDSS3-C	2017-08-18 23:35:20	B	Drout et al. (2017)
VISTA/VIRCAM	2017-08-18 23:44:00	J	Tanvir & Levan (2017)
Magellan-Baade/FourStar	2017-08-18 23:45:49	H	Drout et al. (2017)
PROMPT5(DLT40)/–	2017-08-18 23:47:00	r	Yang et al. (2017b), Valenti et al (submitted)
VLT/FORS2	2017-08-18 23:47:02	Rspecial	Wiersema et al. (2017), Covino et al. (2017)
Swope/DirectCCD	2017-08-18 23:52:29	V	Kilpatrick et al. (2017), Coulter et al. (2017)
VISTA/VIRCAM	2017-08-18 23:53:00	Y	Tanvir & Levan (2017)
TOROS/T80S	2017-08-18 23:53:00	g	Diaz et al. (2017a), Diaz et al. (2017b), Diaz et al (in prepar
TOROS/T80S	2017-08-18 23:53:00	r	Diaz et al. (2017a), Diaz et al. (2017b), Diaz et al (in prepar
TOROS/T80S	2017-08-18 23:53:00	i	Diaz et al. (2017a), Diaz et al. (2017b), Diaz et al (in prepar
MPG2.2m/GROND/–	2017-08-18 23:56:00	i	Smartt et al. (2017)
MPG2.2m/GROND/–	2017-08-18 23:56:00	z	Smartt et al. (2017)
MPG2.2m/GROND/–	2017-08-18 23:56:00	J	Smartt et al. (2017)
MPG2.2m/GROND/–	2017-08-18 23:56:00	r	Smartt et al. (2017)
MPG2.2m/GROND/–	2017-08-18 23:56:00	H	Smartt et al. (2017)
MPG2.2m/GROND/–	2017-08-18 23:56:00	Ks	Smartt et al. (2017)
Gemini-South/Flamingos-2	2017-08-19 00:00:19	H	P. Cowperthwaite et al. (2017)
Magellan-Baade/FourStar	2017-08-19 00:02:53	J1	Drout et al. (2017)
VLT/X-shooter	2017-08-19 00:08:58	r	Pian et al. (2017), Pian et al. (2017)
VLT/X-shooter	2017-08-19 00:10:46	z	Pian et al. (2017), Pian et al. (2017)
VLT/X-shooter	2017-08-19 00:14:01	g	Pian et al. (2017), Pian et al. (2017)
Swift/UVOT	2017-08-19 00:41:00	u	Evans et al. (2017)
Swope/DirectCCD	2017-08-19 00:49:15	B	Kilpatrick et al. (2017), Coulter et al. (2017)
Swope/DirectCCD	2017-08-19 01:08:00	r	Coulter et al. (2017)
NTT/–	2017-08-19 01:09:00	U	Smartt et al. (2017)
Swope/DirectCCD	2017-08-19 01:18:57	g	Coulter et al. (2017)
BOOTES-5/JGT/–	2017-08-19 03:08:14	clear	Castro-Tirado et al. (2017), Zhang et al. (in preparation)
Pan-STARRS1/–	2017-08-19 05:42:00	y	Chambers et al. (2017b), Smartt et al. (2017)
Pan-STARRS1/–	2017-08-19 05:44:00	z	Chambers et al. (2017b), Smartt et al. (2017)
Pan-STARRS1/–	2017-08-19 05:46:00	i	Chambers et al. (2017b), Smartt et al. (2017)
MOA-II/MOA-cam3	2017-08-19 07:26:00	R	Utsumi, Y., et al. (in press)
B&C61cm/Tripole5	2017-08-19 07:26:00	g	Utsumi, Y., et al. (in press)
KMTNet-SSO/wide-fieldcamera	2017-08-19 08:32:48	B	Im et al. (2017d), Im et al. (2017c), Troja et al. (2017)
KMTNet-SSO/wide-fieldcamera	2017-08-19 08:34:43	V	Im et al. (2017d), Im et al. (2017c), Troja et al. (2017)
KMTNet-SSO/wide-fieldcamera	2017-08-19 08:36:39	R	Im et al. (2017d), Im et al. (2017c), Troja et al. (2017)
KMTNet-SSO/wide-fieldcamera	2017-08-19 08:38:42	I	Im et al. (2017d), Im et al. (2017c), Troja et al. (2017)
T27/–	2017-08-19 09:01:31	V	Im et al. (2017a), Im et al. (2017b), Im et al. (in prepara
T30/–	2017-08-19 09:02:27	V	Im et al. (2017a), Im et al. (2017b), Im et al. (in prepara
T27/–	2017-08-19 09:02:27	R	Im et al. (2017a), Im et al. (2017b), Im et al. (in prepara
T31/–	2017-08-19 09:02:34	R	Im et al. (2017a), Im et al. (2017b), Im et al. (in prepara
T27/–	2017-08-19 09:11:30	I	Im et al. (2017a), Im et al. (2017b), Im et al. (in prepara
Zadko/CCDimager	2017-08-19 10:57:00	r	Coward et al. (2017a),
MASTER/–	2017-08-19 17:06:57	Clear	V.M.Lipunov et al. (2017a), Lipunov et al. (2017)
MASTER/–	2017-08-19 17:53:34	R	V.M.Lipunov et al. (2017a), Lipunov et al. (2017)
LasCumbres1-m/Sinistro	2017-08-19 18:01:26	V	Arcavi et al. (2017b)
LasCumbres1-m/Sinistro	2017-08-19 18:01:26	z	Arcavi et al. (2017b)

Table 1 continued

Table 1 *(continued)*

Telescope/Instrument	UT date	Band	References
MASTER/–	2017-08-19 18:04:32	B	V.M.Lipunov et al. (2017a), Lipunov et al. (2017)
1.5B/–	2017-08-19 18:16:00	r	Smartt et al. (2017)
REM/ROS2	2017-08-19 23:12:59	r	Melandri et al. (2017c), Pian et al. (2017)
REM/ROS2	2017-08-19 23:12:59	i	Melandri et al. (2017c), Pian et al. (2017)
REM/ROS2	2017-08-19 23:12:59	g	Melandri et al. (2017c), Pian et al. (2017)
MASTER/–	2017-08-19 23:13:20	Clear	V.M.Lipunov et al. (2017a), Lipunov et al. (2017)
Gemini-South/Flamingos-2	2017-08-19 23:13:34	H	P. Cowperthwaite et al. (2017)
MPG2.2m/GROND/–	2017-08-19 23:15:00	r	Smartt et al. (2017)
MPG2.2m/GROND/–	2017-08-19 23:15:00	z	Smartt et al. (2017)
MPG2.2m/GROND/–	2017-08-19 23:15:00	H	Smartt et al. (2017)
MPG2.2m/GROND/–	2017-08-19 23:15:00	i	Smartt et al. (2017)
MPG2.2m/GROND/–	2017-08-19 23:15:00	J	Smartt et al. (2017)
TOROS/EABA	2017-08-19 23:18:38	r	Diaz et al. (2017b), Diaz et al (in preparation)
Magellan-Baade/FourStar	2017-08-19 23:18:50	H	Drout et al. (2017)
Etelman/VIRT/CCDimager	2017-08-19 23:19:00	R	Gendre et al. (2017), Andreoni et al. (in prep)
Blanco/DECam/–	2017-08-19 23:23:29	Y	P. Cowperthwaite et al. (2017)
Blanco/DECam/–	2017-08-19 23:26:59	r	P. Cowperthwaite et al. (2017)
Blanco/DECam/–	2017-08-19 23:27:59	g	P. Cowperthwaite et al. (2017)
ChilescopeRC-1000/–	2017-08-19 23:30:33	clear	Pozanenko et al. (2017a), Pozanenko et al. (2017b), Pozanenko et al (in p
Magellan-Baade/FourStar	2017-08-19 23:31:06	J1	Drout et al. (2017)
Blanco/DECam/–	2017-08-19 23:31:13	u	P. Cowperthwaite et al. (2017)
Magellan-Baade/FourStar	2017-08-19 23:41:59	Ks	Drout et al. (2017)
Magellan-Baade/IMACS	2017-08-20 00:13:32	r	Drout et al. (2017)
Gemini-South/Flamingos-2	2017-08-20 00:19:00	Ks	Kasliwal et al. (2017)
LasCumbres1-m/Sinistro	2017-08-20 00:24:28	g	Arcavi et al. (2017b)
Gemini-South/Flamingos-2	2017-08-20 00:27:00	J	Kasliwal et al. (2017)
NTT/–	2017-08-20 01:19:00	U	Smartt et al. (2017)
Pan-STARRS1/–	2017-08-20 05:38:00	y	Chambers et al. (2017c), Smartt et al. (2017)
Pan-STARRS1/–	2017-08-20 05:41:00	z	Chambers et al. (2017c), Smartt et al. (2017)
Pan-STARRS1/–	2017-08-20 05:45:00	i	Chambers et al. (2017c), Smartt et al. (2017)
T31/–	2017-08-20 09:20:38	R	Im et al. (2017a), Im et al. (2017b), Im et al. (in prepara
MASTER/–	2017-08-20 17:04:36	Clear	V.M.Lipunov et al. (2017a), Lipunov et al. (2017)
MASTER/–	2017-08-20 17:25:56	R	V.M.Lipunov et al. (2017a), Lipunov et al. (2017)
MASTER/–	2017-08-20 17:36:32	B	V.M.Lipunov et al. (2017a), Lipunov et al. (2017)
LasCumbres1-m/Sinistro	2017-08-20 17:39:50	i	Arcavi et al. (2017b)
LasCumbres1-m/Sinistro	2017-08-20 17:45:36	z	Arcavi et al. (2017b)
LasCumbres1-m/Sinistro	2017-08-20 17:49:55	V	Arcavi et al. (2017b)
MPG2.2m/GROND/–	2017-08-20 23:15:00	g	Smartt et al. (2017)
Magellan-Baade/FourStar	2017-08-20 23:20:42	J	Drout et al. (2017)
ChilescopeRC-1000/–	2017-08-20 23:21:09	clear	Pozanenko et al. (2017a)
VISTA/VIRCAM	2017-08-20 23:24:00	K	Tanvir & Levan (2017)
Blanco/DECam/–	2017-08-20 23:37:06	u	P. Cowperthwaite et al. (2017)
Swope/DirectCCD	2017-08-20 23:44:36	V	Coulter et al. (2017)
Swope/DirectCCD	2017-08-20 23:53:00	B	Coulter et al. (2017)
MASTER/–	2017-08-21 00:26:31	Clear	V.M.Lipunov et al. (2017a), Lipunov et al. (2017)
Gemini-South/Flamingos-2	2017-08-21 00:38:00	H	Kasliwal et al. (2017); Troja et al. (2017)
Pan-STARRS1/–	2017-08-21 05:37:00	y	Chambers et al. (2017d), Smartt et al. (2017)
Pan-STARRS1/–	2017-08-21 05:39:00	z	Chambers et al. (2017d), Smartt et al. (2017)
Pan-STARRS1/–	2017-08-21 05:42:00	i	Chambers et al. (2017d), Smartt et al. (2017)

Table 1 continued

Table 1 *(continued)*

Telescope/Instrument	UT date	Band	References
AST3-2/wide-fieldcamera	2017-08-21 15:36:50	g	–
MASTER/–	2017-08-21 17:08:14	Clear	V.M.Lipunov et al. (2017a), Lipunov et al. (2017)
MASTER/–	2017-08-21 18:06:12	R	V.M.Lipunov et al. (2017a), Lipunov et al. (2017)
MASTER/–	2017-08-21 19:20:23	B	V.M.Lipunov et al. (2017a), Lipunov et al. (2017)
duPont/RetroCam	2017-08-21 23:17:19	Y	Drout et al. (2017)
Etelman/VIRT/CCDimager	2017-08-21 23:19:00	Clear	Gendre et al. (2017), Andreoni et al. (in prep)
MPG2.2m/GROND/–	2017-08-21 23:22:00	Ks	Smartt et al. (2017)
VLT/FORS2	2017-08-21 23:23:11	R	D'Avanzo et al. (2017), Pian et al. (2017)
ChilescopeRC-1000/–	2017-08-21 23:32:09	clear	Pozanenko et al. (2017c)
duPont/RetroCam	2017-08-21 23:34:34	H	Drout et al. (2017)
LasCumbres1-m/Sinistro	2017-08-21 23:48:28	w	Arcavi et al. (2017b)
Swope/DirectCCD	2017-08-21 23:54:57	r	Coulter et al. (2017)
duPont/RetroCam	2017-08-21 23:57:41	J	Drout et al. (2017)
Swope/DirectCCD	2017-08-22 00:06:17	g	Coulter et al. (2017)
VLT/FORS2	2017-08-22 00:09:09	z	D'Avanzo et al. (2017), Pian et al. (2017)
VLT/FORS2	2017-08-22 00:18:49	I	D'Avanzo et al. (2017), Pian et al. (2017)
Magellan-Clay/LDSS3-C	2017-08-22 00:27:40	g	Drout et al. (2017)
VLT/FORS2	2017-08-22 00:28:18	B	D'Avanzo et al. (2017), Pian et al. (2017)
VLT/FORS2	2017-08-22 00:38:20	V	D'Avanzo et al. (2017), Pian et al. (2017)
HST/WFC3/IR	2017-08-22 07:34:00	F110W	Tanvir & Levan (2017), Troja et al. (2017)
LasCumbres1-m/Sinistro	2017-08-22 08:35:31	r	Arcavi et al. (2017b)
HST/WFC3/IR	2017-08-22 10:45:00	F160W	Tanvir & Levan (2017), Troja et al. (2017)
HubbleSpaceTelescope/WFC3	2017-08-22 20:19:00	F336W	Adams et al. (2017), Kasliwal et al. (2017)
Etelman/VIRT/CCDimager	2017-08-22 23:19:00	Clear	Gendre et al. (2017), Andreoni et al. (in prep)
VLT/VIMOS	2017-08-22 23:30:00	z	Tanvir & Levan (2017)
duPont/RetroCam	2017-08-22 23:33:54	Y	Drout et al. (2017)
VLT/VIMOS	2017-08-22 23:42:00	R	Tanvir & Levan (2017)
VLT/VIMOS	2017-08-22 23:53:00	u	Evans et al. (2017)
VLT/FORS2	2017-08-22 23:53:31	Rspecial	Covino et al. (2017)
VST/OmegaCam	2017-08-22 23:58:32	g	Grado et al. (2017a), Pian et al. (2017)
VLT/X-shooter	2017-08-23 00:35:20	r	Pian et al. (2017)
VLT/X-shooter	2017-08-23 00:37:08	z	Pian et al. (2017)
VLT/X-shooter	2017-08-23 00:40:24	g	Pian et al. (2017)
Zadko/CCDimager	2017-08-23 11:32:00	r	Coward et al. (2017a),
IRSF/SIRIUS	2017-08-23 17:22:00	Ks	Kasliwal et al. (2017)
IRSF/SIRIUS	2017-08-23 17:22:00	J	Kasliwal et al. (2017)
IRSF/SIRIUS	2017-08-23 17:22:00	H	Kasliwal et al. (2017)
VST/OmegaCam	2017-08-23 23:26:51	i	Grado et al. (2017a), Pian et al. (2017)
VLT/VISIR	2017-08-23 23:35:00	8.6um	Kasliwal et al. (2017)
VST/OmegaCam	2017-08-23 23:42:49	r	Grado et al. (2017a), Pian et al. (2017)
CTIO1.3m/ANDICAM	2017-08-24 23:20:00	Ks	Kasliwal et al. (2017)
Swope/DirectCCD	2017-08-24 23:45:07	i	Coulter et al. (2017)
ChilescopeRC-1000/–	2017-08-24 23:53:39	clear	Pozanenko et al. (2017b),
Blanco/DECam/–	2017-08-24 23:56:22	g	P. Cowperthwaite et al. (2017)
Magellan-Clay/LDSS3-C	2017-08-25 00:43:27	B	Drout et al. (2017)
HST/WFC3/UVIS	2017-08-25 13:55:00	F606W	Tanvir & Levan (2017), Troja et al. (2017)
HST/WFC3/UVIS	2017-08-25 15:28:00	F475W	Tanvir & Levan (2017), Troja et al. (2017)
HST/WFC3/UVIS	2017-08-25 15:36:00	F275W	Levan & Tanvir (2017), Tanvir & Levan (2017),
Magellan-Clay/LDSS3-C	2017-08-25 23:19:41	z	Drout et al. (2017)
Blanco/DECam/–	2017-08-25 23:56:05	r	P. Cowperthwaite et al. (2017)

Table 1 continued

Table 1 *(continued)*

Telescope/Instrument	UT date	Band	References
VLT/FORS2	2017-08-26 00:13:40	z	Covino et al. (2017)
duPont/RetroCam	2017-08-26 00:14:28	J	Drout et al. (2017)
VLT/FORS2	2017-08-26 00:27:16	B	Pian et al. (2017)
IRSF/SIRIUS	2017-08-26 16:57:00	J	Kasliwal et al. (2017)
IRSF/SIRIUS	2017-08-26 16:57:00	Ks	Kasliwal et al. (2017)
IRSF/SIRIUS	2017-08-26 16:57:00	H	Kasliwal et al. (2017)
VISTA/VIRCAM	2017-08-26 23:38:00	Y	Tanvir & Levan (2017)
ApachePointObservatory/NICFPS	2017-08-27 02:15:00	Ks	Kasliwal et al. (2017)
Palomar200inch/WIRC	2017-08-27 02:49:00	Ks	Kasliwal et al. (2017)
HST/WFC3/IR	2017-08-27 06:45:56	F110W	P. Cowperthwaite et al. (2017)
HST/WFC3/IR	2017-08-27 07:06:57	F160W	P. Cowperthwaite et al. (2017)
HST/WFC3/UVIS	2017-08-27 08:20:49	F336W	P. Cowperthwaite et al. (2017)
HST/ACS/WFC	2017-08-27 10:24:14	F475W	P. Cowperthwaite et al. (2017)
HST/ACS/WFC	2017-08-27 11:57:07	F625W	P. Cowperthwaite et al. (2017)
HST/ACS/WFC	2017-08-27 13:27:15	F775W	P. Cowperthwaite et al. (2017)
HST/ACS/WFC	2017-08-27 13:45:24	F850LP	P. Cowperthwaite et al. (2017)
Gemini-South/Flamingos-2	2017-08-27 23:16:00	J	Kasliwal et al. (2017)
CTIO1.3m/ANDICAM	2017-08-27 23:18:00	Ks	Kasliwal et al. (2017)
Blanco/DECam/–	2017-08-27 23:23:33	Y	P. Cowperthwaite et al. (2017)
MPG2.2m/GROND/–	2017-08-27 23:24:00	J	Smartt et al. (2017)
Gemini-South/Flamingos-2	2017-08-27 23:28:10	K_s	P. Cowperthwaite et al. (2017)
Gemini-South/Flamingos-2	2017-08-27 23:33:07	H	P. Cowperthwaite et al. (2017)
duPont/RetroCam	2017-08-27 23:36:25	H	Drout et al. (2017)
Blanco/DECam/–	2017-08-27 23:40:57	z	P. Cowperthwaite et al. (2017)
Blanco/DECam/–	2017-08-28 00:00:01	i	P. Cowperthwaite et al. (2017)
VLT/FORS2	2017-08-28 00:07:31	R	Pian et al. (2017)
VLT/FORS2	2017-08-28 00:15:56	V	Pian et al. (2017)
MPG2.2m/GROND/–	2017-08-28 00:22:00	H	Smartt et al. (2017)
HST/WFC3/IR	2017-08-28 01:50:00	F110W	Tanvir & Levan (2017), Troja et al. (2017)
HST/WFC3/IR	2017-08-28 03:25:00	F160W	Tanvir & Levan (2017), Troja et al. (2017)
HST/WFC3/UVIS	2017-08-28 20:56:00	F275W	Levan & Tanvir (2017), Tanvir & Levan (2017),
HST/WFC3/UVIS	2017-08-28 22:29:00	F475W	Tanvir & Levan (2017), Troja et al. (2017)
HST/WFC3/UVIS	2017-08-28 23:02:00	F814W	Tanvir & Levan (2017), Troja et al. (2017)
NTT/–	2017-08-28 23:03:00	H	Smartt et al. (2017)
HST/WFC3/UVIS	2017-08-28 23:08:00	F606W	Tanvir & Levan (2017), Troja et al. (2017)
MPG2.2m/GROND/–	2017-08-28 23:22:00	Ks	Smartt et al. (2017)
VISTA/VIRCAM	2017-08-28 23:33:00	J	Tanvir & Levan (2017)
Gemini-South/Flamingos-2	2017-08-28 23:36:01	K_s	P. Cowperthwaite et al. (2017)
VLT/FORS2	2017-08-29 00:00:13	I	Pian et al. (2017)
HubbleSpaceTelescope/WFC3/UVIS	2017-08-29 00:36:00	F275W	Kasliwal et al. (2017)
HubbleSpaceTelescope/WFC3/UVIS	2017-08-29 00:36:00	F225W	Kasliwal et al. (2017)
NTT/–	2017-08-29 22:56:00	Ks	Smartt et al. (2017)
VLT/VIMOS	2017-08-29 23:16:00	R	Tanvir & Levan (2017)
SkyMapper/–	2017-08-30 09:26:00	u	–
SkyMapper/–	2017-08-30 09:32:00	v	–
NTT/–	2017-08-30 23:03:00	Ks	Smartt et al. (2017)
VLT/FORS2	2017-08-31 23:34:46	z	Pian et al. (2017)
VISTA/VIRCAM	2017-08-31 23:42:00	K	Tanvir & Levan (2017)
Gemini-South/Flamingos-2	2017-08-31 23:50:00	H	Singer et al. (2017b), Kasliwal et al. (2017)
SkyMapper/–	2017-09-01 09:12:00	i	–

Table 1 continued

Table 1 *(continued)*

Telescope/Instrument	UT date	Band	References
SkyMapper/–	2017-09-01 09:14:00	z	–
SkyMapper/–	2017-09-03 09:21:00	g	–
SkyMapper/–	2017-09-03 09:23:00	r	–
NTT/–	2017-09-04 23:12:00	Ks	Smartt et al. (2017)
Gemini-South/Flamingos-2	2017-09-04 23:28:45	K_s	P. Cowperthwaite et al. (2017)
VLT/VIMOS	2017-09-05 23:23:00	z	Tanvir & Levan (2017)
Gemini-South/Flamingos-2	2017-09-05 23:48:00	Ks	Kasliwal et al. (2017)
Magellan-Baade/FourStar	2017-09-06 23:24:28	Ks	Drout et al. (2017)
VLT/HAWKI	2017-09-07 23:11:00	K	Tanvir & Levan (2017)
VLT/HAWKI	2017-09-11 23:21:00	K	Tanvir & Levan (2017)

Table 2. Record of spectral observations.

Telescope/Instrument	UT date	Wavelengths (Å)	Resolution (R)	References
Magellan-Clay/LDSS-3	2017-08-18 00:26:17	3780-10200	860	Drout et al. (2017), Shappee et al. (2017)
Magellan-Clay/LDSS-3	2017-08-18 00:40:09	3800-6200	1900	Shappee et al. (2017)
Magellan-Clay/LDSS-3	2017-08-18 00:52:09	6450-10000	1810	Shappee et al. (2017)
Magellan-Baade/MagE	2017-08-18 01:26:22	3650-10100	5800	Shappee et al. (2017)
ANU2.3/WiFeS	2017-08-18 09:24:00	3200-9800	B/R 3000	–
SALT/RSS	2017-08-18 17:07:00	3600-8000	300	Shara et al. (2017),
NTT/EFOSC2Gr#11+16	2017-08-18 23:19:12	3330-9970	260/400	Smartt et al. (2017)
VLT/X-shooter	2017-08-18 23:22:25	3000-24800	4290/8150/5750	Pian et al. (2017), Pian et al. (2017)
SOAR/GHTS	2017-08-18 23:22:39	4000–8000	830	Nicholl et al. (2017)
Magellan-Clay/LDSS-3	2017-08-18 23:47:37	3820-9120	860	Shappee et al. (2017)
VLT/MUSE	2017-08-18 23:49:00	4650-9300	3000	Levan & Tanvir (2017), Tanvir & Levan (2017)
Magellan-Clay/MIKE	2017-08-19 00:18:11	3900-9400	30000	Shappee et al. (2017)
Magellan-Baade/MagE	2017-08-19 00:35:25	3800-10300	4100	Shappee et al. (2017)
Gemini-South/FLAMINGOS2	2017-08-19 00:42:27	9100–18000	500	R. Chornock et al. (2017)
LCOFaulkesTelescopeSouth/FLOYDS	2017-08-19 08:36:22	5500-9250	700	GC21908, McCully et al. (2017)
ANU2.3/WiFeS	2017-08-19 09:26:12	3200-9800	B/R 3000	–
SALT/RSS	2017-08-19 16:58:00	3600-8000	300	Shara et al. (2017),
SALT/RSS	2017-08-19 16:58:32	3600-8000	300	Shara et al. (2017), Shara et al. 2017, McCully et al. (2017)
NTT/EFOSC2Gr#11+16	2017-08-19 23:25:41	3330-9970	260/400	Smartt et al. (2017)
SOAR/GHTS	2017-08-19 23:28:32	4000–8000	830	Nicholl et al. (2017)
VLT/Xshooterfixed	2017-08-19 23:28:46	3700-22790	4290/3330/5450	Smartt et al. (2017)
Gemini-South/FLAMINGOS2	2017-08-19 23:42:56	9100–18000	500	R. Chornock et al. (2017)
Magellan-Baade/IMACS	2017-08-20 00:26:28	4355-8750	1000	Shappee et al. (2017)
GeminiSouth/GMOS	2017-08-20 01:01:54	4000-9500	400	McCully et al. (2017), McCully et al. (2017)
Gemini-South/GMOS	2017-08-20 01:08:00	6000-9000	1900	Kasliwal et al. (2017)
ANU2.3/WiFeS	2017-08-20 09:21:33	3200-9800	B/R 3000	–
NTT/EFOSC2Gr#11+16	2017-08-20 23:21:13	3330-9970	390/600	Smartt et al. (2017)
SOAR/GHTS	2017-08-20 23:23:17	5000–9000	830	Nicholl et al. (2017)
VLT/X-shooter	2017-08-20 23:25:28	3000-24800	4290/8150/5750	Pian et al. (2017)
Magellan-Clay/LDSS-3	2017-08-20 23:45:53	4450-10400	860	Shappee et al. (2017)
Gemini-South/GMOS	2017-08-21 00:15:00	3800-9200	1700	Troja et al. (2017a), Kasliwal et al. (2017), Troja et al. (2017)
GeminiSouth/GMOS	2017-08-21 00:16:09	4000-9500	400	Troja et al. (2017a), McCully et al. (2017), Troja et al. (2017)
VLT/FORS2	2017-08-21 00:43:12	3500-8600	800-1000	Pian et al. (2017)
ANU2.3/WiFeS	2017-08-21 09:13:00	3200-7060	B 3000 R 7000	–

Table 2 continued

Table 2 *(continued)*

Telescope/Instrument	UT date	Wavelengths (Å)	Resolution (R)	References
NTT/SOFIBlueGrism	2017-08-21 23:11:37	9380-16460	550	Smartt et al. (2017)
SOAR/GHTS	2017-08-21 23:24:49	4000–8000	830	Nicholl et al. (2017)
VLT/Xshooterfixed	2017-08-21 23:25:38	3700-22790	4290/3330/5450	Smartt et al. (2017)
VLT/FORS2	2017-08-21 23:31:12	3500-8600	800-1000	Pian et al. (2017)
Gemini-South/FLAMINGOS2	2017-08-21 23:40:09	9100–18000	500	R. Chornock et al. (2017)
Gemini-South/Flamingos-2	2017-08-22 00:21:00	12980-25070	600	Kasliwal et al. (2017)
Gemini-South/Flamingos-2	2017-08-22 00:47:00	9840-18020	600	Kasliwal et al. (2017)
Magellan-Clay/LDSS-3	2017-08-22 00:50:34	5010-10200	860	Shappee et al. (2017)
HST/WFC3/IR-G102	2017-08-22 09:07:00	8000-11150	210	Tanvir & Levan (2017), Troja et al. (2017)
HST/WFC3/IR-G141	2017-08-22 10:53:00	10750-17000	130	Tanvir & Levan (2017), Troja et al. (2017)
Magellan-Clay/LDSS-3	2017-08-22 23:34:00	5000-10200	860	Shappee et al. (2017)
HST/STIS	2017-08-23 02:51:54	1600–3200	700	Nicholl et al. (2017)
AAT/AAOmega+2DF	2017-08-24 08:55:00	3750-8900	1700	Andreoni et al. (2017),
HST/WFC3/IR-G102	2017-08-24 18:58:00	8000-11150	210	Tanvir & Levan (2017), Troja et al. (2017)
Magellan-Clay/LDSS-3	2017-08-24 23:33:51	6380-10500	1810	Shappee et al. (2017)
SOAR/GHTS	2017-08-24 23:34:31	5000–9000	830	Nicholl et al. (2017)
Gemini-South/FLAMINGOS2	2017-08-24 23:56:32	9100–18000	500	R. Chornock et al. (2017)
KeckI/LRIS	2017-08-25 05:45:00	2000-10300	1000	Kasliwal et al. (2017)
Magellan/Baade/IMACS	2017-08-25 23:37:59	4300–9300	1100	Nicholl et al. (2017)
Magellan-Clay/LDSS-3	2017-08-25 23:39:18	6380-10500	1810	Shappee et al. (2017)
Gemini-South/FLAMINGOS2	2017-08-26 00:21:24	9100–18000	500	R. Chornock et al. (2017)
HST/WFC3/IR-G141	2017-08-26 22:57:00	10750-17000	130	Tanvir & Levan (2017), Troja et al. (2017)
Magellan/Baade/IMACS	2017-08-26 23:20:54	4300–9300	1100	Nicholl et al. (2017)
Gemini-South/FLAMINGOS2	2017-08-27 00:12:20	9100–18000	500	R. Chornock et al. (2017)
Gemini-South/FLAMINGOS2	2017-08-28 00:16:28	9100–18000	500	R. Chornock et al. (2017)
HST/WFC3/IR-G102	2017-08-28 01:58:00	8000-11150	210	Tanvir & Levan (2017), Troja et al. (2017)
HST/WFC3/IR-G141	2017-08-28 03:33:00	10750-17000	130	Tanvir & Levan (2017), Troja et al. (2017)
Gemini-South/Flamingos-2	2017-08-29 00:23:00	12980-25070	600	Kasliwal et al. (2017)

[a] Assuming no shielding by the structures of ISS.

Table 3. Gamma-ray Monitoring and Evolution of GW 170817

Observatory	UT date	Time since GW trigger	90% Flux upper limit ($\mathrm{erg\,cm^{-2}\,s^{-1}}$)	Energy band	GCN/Reference
CALET CGBM	Aug 17 12:41:04 UTC	0.0	1.3×10^{-7} [a]	10–1000 keV	Nakahira et al. (2017)
Konus-*Wind*	Aug 17 12:41:04.446 UTC	0.0	3.0×10^{-7} [erg/cm^2]	10 keV–10 MeV	Svinkin et al. (2017a)
Insight-HXMT/HE	Aug 17 12:34:24 UTC	-400 s	3.7×10^{-7}	0.2–5 MeV	Li et al. (2017)
Insight-HXMT/HE	Aug 17 12:41:04.446 UTC	0.0	3.7×10^{-7}	0.2–5 MeV	Li et al. (2017)
Insight-HXMT/HE	Aug 17 12:41:06.30 UTC	1.85 s	6.6×10^{-7}	0.2–5 MeV	Li et al. (2017)
Insight-HXMT/HE	Aug 17 12:46:04 UTC	300 s	1.5×10^{-7}	0.2–5 MeV	Li et al. (2017)
AGILE-GRID	Aug 17 12:56:41 UTC	0.011 d	3.9×10^{-9}	0.03-3 GeV	Verrecchia et al. (2017)
Fermi-LAT	Aug 17 13:00:14 UTC	0.013 d	4.0×10^{-10}	0.1–1 GeV	Kocevski et al. (2017)
H.E.S.S.	Aug 17 17:59 UTC	0.22 d	3.9×10^{-12}	0.28–2.31 TeV	Abdalla, H. et al. (H.E.S.S. Collaboration) (2017)
HAWC	Aug 17 20:53:14 – Aug 17 22:55:00 UTC	0.342 d + 0.425 d	1.7×10^{-10}	4–100 TeV	Martinez-Castellanos et al. (2017)
Fermi-GBM	Aug 16 12:41:06 – Aug 18 12:41:06 UTC	$\pm$ 1.0 d	$(8.0 - 9.9) \times 10^{-10}$	20-100 keV	Goldstein et al. (2017)
NTEGRAL IBIS/ISGRI	Aug 18 12:45:10 – Aug 23 03:22:34 UTC	1–5.7 d	2.0×10^{-11}	20–80 keV	Savchenko et al. (2017)
INTEGRAL IBIS/ISGRI	Aug 18 12:45:10 – Aug 23 03:22:34 UTC	1–5.7 d	3.6×10^{-11}	80–300 keV	Savchenko et al. (2017)
INTEGRAL IBIS/PICsIT	Aug 18 12:45:10 – Aug 23 03:22:34 UTC	1–5.7 d	0.9×10^{-10}	468–572 keV	Savchenko et al. (2017)
INTEGRAL IBIS/PICsIT	Aug 18 12:45:10 – Aug 23 03:22:34 UTC	1–5.7 d	4.4×10^{-10}	572–1196 keV	Savchenko et al. (2017)
INTEGRAL SPI	Aug 18 12:45:10 – Aug 23 03:22:34 UTC	1–5.7 d	2.4×10^{-10}	300–500 keV	Savchenko et al. (2017)
INTEGRAL SPI	Aug 18 12:45:10 – Aug 23 03:22:34 UTC	1–5.7 d	7.0×10^{-10}	500–1000 keV	Savchenko et al. (2017)
INTEGRAL SPI	Aug 18 12:45:10 – Aug 23 03:22:34 UTC	1–5.7 d	1.5×10^{-9}	1000–2000 keV	Savchenko et al. (2017)
INTEGRAL SPI	Aug 18 12:45:10 – Aug 23 03:22:34 UTC	1–5.7 d	2.9×10^{-9}	2000–4000 keV	Savchenko et al. (2017)
H.E.S.S.	Aug 18 17:55 UTC	1.22 d	3.3×10^{-12}	0.27–3.27 TeV	Abdalla, H. et al. (H.E.S.S. Collaboration) (2017)
H.E.S.S.	Aug 19 17:56 UTC	2.22 d	1.0×10^{-12}	0.31–2.88 TeV	Abdalla, H. et al. (H.E.S.S. Collaboration) (2017)
H.E.S.S.	Aug 21 + Aug 22 18:15 UTC	4.23 d + 5.23 d	2.9×10^{-12}	0.50–5.96 TeV	Abdalla, H. et al. (H.E.S.S. Collaboration) (2017)

Table 4. X-ray Monitoring and Evolution of GW 170817

Observatory	UT date (start)	Time since GW trigger (days)	f_x (erg cm^{-2} s^{-1})	L_x (erg/s)	Energy (keV)	GCN/Reference
MAXI	Aug 17 17:21:54 UTC	0.19	$<8.6\times10^{-9}$	$<1.65\times10^{45}$	2–10	Sugita et al. (in prep.)
MAXI	Aug 17 18:54:27 UTC	0.26	$<7.7\times10^{-8}$	$<1.47\times10^{46}$	2–10	Sugita et al. (in prep.)
MAXI	Aug 18 00:44:59 UTC	0.50	$<4.2\times10^{-9}$	$<8.0\times10^{44}$	2–10	Sugita et al. (in prep.)
Super-*AGILE*	Aug 18 01:16:34 UTC	0.53	$< 3.0 \times 10^{-9}$	$< 5.4 \times 10^{44}$	18–60	Verrecchia et al. (2017)
MAXI	Aug 18 02:18:08 UTC	0.57	$<2.2\times10^{-9}$	$<4.2\times10^{44}$	2–10	Sugita et al. (in prep.)
Swift-XRT	Aug 18 03:34:33 UTC	0.62	$< 2.74 \times 10^{-13}$	$< 5.25 \times 10^{40}$	0.3–10	Evans et al. (2017)
NuSTAR	Aug 18 05:25 UTC	0.7	$< 2.62 \times 10^{-14}$	$< 5.01 \times 10^{39}$	3–10	Evans et al. (2017)
Swift-XRT	Aug 18 12:11:49 UTC	0.98	$< 2.62 \times 10^{-12}$	$< 5.01 \times 10^{41}$	0.3–10	Evans et al. (2017)
INTEGRAL JEM-X	Aug 18 12:45:10 UTC	1–5.7	$< 1.9 \times 10^{-11}$	$< 3.6 \times 10^{42}$	3–10	Savchenko et al. (2017)
INTEGRAL JEM-X	Aug 18 12:45:10 UTC	1–5.7	$< 7.0 \times 10^{-12}$	$< 1.3 \times 10^{42}$	10–25	Savchenko et al. (2017)
Swift-XRT	Aug 18 13:29:43 UTC	1.03	$< 1.77 \times 10^{-13}$	$< 3.39 \times 10^{40}$	0.3–10	Evans et al. (2017)
Swift-XRT	Aug 19 00:18:22 UTC	1.48	$< 1.31 \times 10^{-13}$	$< 2.51 \times 10^{40}$	0.3–10	Evans et al. (2017)
Chandra	Aug 19 17:10:09 UTC	2.20	non-detection	...	0.3-10	Margutti et al. (2017)
Swift-XRT	Aug 19 13:24:05 UTC	2.03	$< 1.02 \times 10^{-13}$	$< 1.95 \times 10^{40}$	0.3–10	Evans et al. (2017)
Swift-XRT	Aug 19 18:30:52 UTC	2.24	$< 1.34 \times 10^{-13}$	$< 2.57 \times 10^{40}$	0.3–10	Evans et al. (2017)
Swift-XRT	Aug 20 03:24:44 UTC	2.61	$< 1.41 \times 10^{-13}$	$< 2.69 \times 10^{40}$	0.3–10	Evans et al. (2017)
Swift-XRT	Aug 20 08:28:05 UTC	2.82	$< 3.87 \times 10^{-14}$	$< 7.41 \times 10^{39}$	0.3–10	Evans et al. (2017)
Swift-XRT	Aug 21 01:43:44 UTC	3.54	$< 6.73 \times 10^{-14}$	$< 1.29 \times 10^{40}$	0.3–10	Evans et al. (2017)
NuSTAR	Aug 21 20:45:00 UTC	4.3	$< 2.08 \times 10^{-14}$	$< 3.98 \times 10^{39}$	3–10	Evans et al. (2017)
Swift-XRT	Aug 22 00:05:57 UTC	4.48	$< 6.28 \times 10^{-14}$	$< 1.20 \times 10^{40}$	0.3–10	Evans et al. (2017)
Swift-XRT	Aug 23 06:22:57 UTC	5.74	$< 6.89 \times 10^{-14}$	$< 1.32 \times 10^{40}$	0.3–10	Evans et al. (2017)
Swift-XRT	Aug 23 23:59:57 UTC	6.47	$< 7.21 \times 10^{-14}$	$< 1.38 \times 10^{40}$	0.3–10	Evans et al. (2017)
Chandra	Aug 26 10:33:50 UTC	8.9	Detection	...	0.5-8.0	Troja et al. (2017a); Troja et al. (2017)
Swift-XRT	Aug 26 23:59:57 UTC	9.47	$< 8.67 \times 10^{-14}$	$< 1.66 \times 10^{40}$	0.3–10	Evans et al. (2017)
Swift-XRT	Aug 28 10:46:17 UTC	10.92	$< 1.41 \times 10^{-13}$	$< 2.69 \times 10^{40}$	0.3–10	Evans et al. (2017)
Swift-XRT	Aug 29 01:04:57 UTC	11.52	$< 6.00 \times 10^{-14}$	$< 1.15 \times 10^{40}$	0.3–10	Evans et al. (2017)
Swift-XRT	Aug 30 01:00:57 UTC	12.51	$< 5.47 \times 10^{-14}$	$< 1.05 \times 10^{40}$	0.3–10	Evans et al. (2017)
Swift-XRT	Aug 31 02:27:52 UTC	13.57	$< 3.87 \times 10^{-14}$	$< 7.41 \times 10^{39}$	0.3–10	Evans et al. (2017)
Swift-XRT	Sep 01 05:53:04 UTC	14.72	$< 4.45 \times 10^{-14}$	$< 8.51 \times 10^{39}$	0.3–10	Evans et al. (2017)
Chandra	Sep 01 15:22:22 UTC	15.1		...	...	Fong et al. (2017); R. Margutti et al. (2017)
Chandra	Sep 01 15:22:22 UTC	15.1	4.5×10^{-15}	9×10^{38}	0.5-8.0	Troja et al. (2017b); Troja et al. (2017)
Chandra	Sep 02 15:22:22 UTC	15.1	3.5×10^{-15}	2.7×10^{38}	0.3-10	Haggard et al. (2017b,a)
Chandra	Sep 02 00:00:00 UTC	16.1	3.8×10^{-15}	3.0×10^{38}	0.3-10	Haggard et al. (2017b,a)
Swift-XRT	Sep 02 08:40:56 UTC	15.83	$< 1.51 \times 10^{-13}$	$< 2.88 \times 10^{40}$	0.3–10	Evans et al. (2017)
NuSTAR	Sep 04 17:56 UTC	18.2	$< 6.58 \times 10^{-14}$	$< 1.26 \times 10^{40}$	3–10	Evans et al. (2017)
NuSTAR	Sep 05 14:51 UTC	19.1	$< 4.15 \times 10^{-14}$	$< 7.94 \times 10^{39}$	3–10	Evans et al. (2017)
NuSTAR	Sep 06 17:56 UTC	20.1	$< 3.30 \times 10^{-14}$	$< 6.31 \times 10^{39}$	3–10	Evans et al. (2017)
NuSTAR	Sep 21 11:10 UTC	34.9	$< 1.65 \times 10^{-14}$	$< 3.16 \times 10^{39}$	3–10	Evans et al. (2017)

Table 5. Radio Monitoring and Evolution of GW 170817

Telescope	UT date	Time since GW trigger (days)	Central frequency (GHz)	Bandwidth (GHz)	Flux (μ Jy), 3 σ	GCN/Reference
LWA1	Aug 17 13:09:51 UTC	0.02	0.02585	0.020		Callister et al. (2017a)
LWA1	Aug 17 13:09:51 UTC	0.02	0.04545	0.020		Callister et al. (2017a)
LWA1	Aug 17 19:15:00 UTC	0.27	0.02585	0.020		Callister et al. (2017a)
LWA1	Aug 17 19:15:00 UTC	0.27	0.04545	0.020		Callister et al. (2017a)
VLBA	Aug 17 19:58:00 UTC	0.30	8.7	0.26		Deller et al. (2017a)
VLA	Aug 18 02:18:00 UTC	0.57	10.0	-		Alexander et al. (2017a,b)
ATCA	Aug 18 01:00:00 UTC	1	8.5	2.049	< 120	Bannister et al. (2017c)
						Kaplan et al. (2017a)
						Hallinan, Corsi et al. (2017)
ATCA	Aug 18 01:00:00 UTC	1	10.5	2.049	< 150	Bannister et al. (2017c)
						Kaplan et al. (2017a)
						Hallinan, Corsi et al. (2017)
ATCA	Aug 18 01:00:00 UTC	1	16.7	2.049	< 130	Kaplan et al. (2017a)
						Hallinan, Corsi et al. (2017)
ATCA	Aug 18 01:00:00 UTC	1	21.2	2.049	< 140	Kaplan et al. (2017a)
						Hallinan, Corsi et al. (2017)
VLITE	Aug 18 22:23:31 UTC	1.44	0.3387	0.034	$<$34800	Hallinan, Corsi et al. (2017)
ASKAP	Aug 18 04:05:35 UTC	0.67	1.34	0.19		Bannister et al. (2017d,b)
MWA	Aug 18 07:07:50 UTC	1	0. 185	0.03	$< 51\,000$	Kaplan et al. (2017b)
ASKAP	Aug 18 08:57:33 UTC	0.86	1.34	0.19		Bannister et al. (2017d,b)
VLA	Aug 18 22:04:57 UTC	1	10.0	3.8	< 17.0	Alexander et al. (2017c)
ALMA	Aug 18 22:50:40 UTC	1.4	338.5	7.5	–	Schulze et al. (2017)
GMRT	Aug 18 11:00:00 UTC	1	10.0	0.032	< 195	De et al. (2017a)
						Hallinan, Corsi et al. (2017)
Parkes	Aug 18 00:00:00 UTC	1.38	1.34	0.34	$< 1.4 \times 10^6$	Bailes et al. (2017a)
Parkes	Aug 18 00:00:00 UTC	1.46	1.34	0.34	$< 1.4 \times 10^6$	Bailes et al. (2017a)
ASKAP	Aug 19 02:08:00 UTC	1.58	1.34	0.19		Bannister et al. (2017d,b)
ASKAP	Aug 19 05:34:33 UTC	2	1.345	-	< 900	Dobie et al. (2017a)
VLA	Aug 19 22:01:48 UTC	2	6.0	4	< 22	Corsi et al. (2017a)
VLA	Aug 19 22:01:48 UTC	2	6.0	4	< 22	Corsi et al. (2017a)
VLITE	Aug 19 22:29:29 UTC	2.44	0.3387	0.034	$<$28800	Hallinan, Corsi et al. (2017)
VLA	Aug 19 22:30:10 UTC	2.42	15.0	6	< 22	Corsi et al. (2017e)
						Hallinan, Corsi et al. (2017)
VLA	Aug 19 23:04:06 UTC	2.44	10.0	4	< 17	Corsi et al. (2017b)
						Hallinan, Corsi et al. (2017)
VLA	Aug 19 23:33:30 UTC	2.46	6.0	-	< 20	Corsi et al. (2017a)
						Hallinan, Corsi et al. (2017)
ALMA	Aug 19 22:31:43 UTC	2	97.5	-	< 50	Williams et al. (2017a)
Parkes	Aug 20 00:00:00 UTC	3.17	1.34	0.34	$< 1.4 \times 10^6$	Bailes et al. (2017a)
Parkes	Aug 20 00:00:00 UTC	3.21	1.34	0.34	$< 1.4 \times 10^6$	Bailes et al. (2017a)
VLITE	Aug 20 20.49:36 UTC	3.34	0.3387	0.034	$<$44700	Hallinan, Corsi et al. (2017)
VLA	Aug 20 00:01:24 UTC	3	9.7	4	< 18	Corsi et al. (2017b)
GMRT	Aug 20 08:00:00 UTC	3	0.4	0.2	< 780	De et al. (2017b)
GMRT	Aug 20 08:00:00 UTC	3	1.2	0.4	< 98	De et al. (2017b)
VLA	Aug 20 21:07:00 UTC	3	6.2	4	< 19	Corsi et al. (2017c)
VLA/JAGWAR	Aug 20 22:20:00 UTC	3	3.0	-	< 32	Mooley et al. (2017a)

Table 5 continued

Table 5 *(continued)*

Telescope	UT date	Time since GW trigger (days)	Central frequency (GHz)	Bandwidth (GHz)	Flux (μ Jy), 3 σ	GCN/Reference
ATCA	Aug 20 23:31:03 UTC	3	8.5	2.049	< 20	Lynch et al. (2017a)
ATCA	Aug 20 23:31:03 UTC	3	10.5	2.049	< 135	Lynch et al. (2017a)
ALMA	Aug 20 22:40:16 UTC	3	338.5	7.5	–	Schulze et al. (2017)
VLBA	Aug 20 21:36:00 UTC	3	8.7	-	< 48	Deller et al. (2017b)
ALMA	Aug 21 20:58:51 UTC	4.3	338.5	7.5	–	Schulze et al. (2017)
VLA	Aug 22 23:50:18 UTC	5.48	10.0	-		K. Alexander et al. (2017)
e-MERLIN	Aug 23 12:00:00 UTC	6	5.0	0.512	< 108	Moldon et al. (2017a)
e-MERLIN	Aug 24 12:00:00 UTC	7	5.0	0.512	< 96	Moldon et al. (2017a)
LWA1	Aug 24 19:50:00 UTC	7	0.02585	0.016		Callister et al. (2017b)
LWA1	Aug 24 19:50:00 UTC	7	0.04545	0.016		Callister et al. (2017b)
e-MERLIN	Aug 25 12:00:00 UTC	8	5.0	512	< 96	Moldon et al. (2017a)
VLITE	Aug 25 20:38:22 UTC	8.37	0.3387	0.034	< 37500	Hallinan, Corsi et al. (2017)
GMRT	Aug 25 09:30:00 UTC	7.9	1.39	0.032	< 130	Resmi et al. (2017)
VLA	Aug 25 19:15:12 UTC	8.29	10.0	-		K. Alexander et al. (2017)
ALMA	Aug 25 22:35:17 UTC	8.4	338.5	7.5	–	Schulze et al. (2017)
MeerKAT	Aug 26 08:43:00 UTC	10	1.48	0.22	< 70	Goedhart et al. (2017a)
ALMA	Aug 26 22:49:25 UTC	9.43	97.5	-		Williams et al. (2017a)
ALMA	Aug 26 22:58:41 UTC	9.4	338.5	7.5	–	Schulze et al. (2017); Kim et al. (2017)
EVN	Aug 26 12:15:00 UTC	9	5.0	0.256	<96	Paragi et al. (2017a)
e-MERLIN	Aug 26 12:00:00 UTC	9	5.0	0.512	< 114	Moldon et al. (2017a)
e-MERLIN	Aug 27 12:00:00 UTC	10	5.0	0.512	< 90	Moldon et al. (2017a)
ATCA	Aug 27 23:26:25 UTC	10	8.5	2. 049	< 54	Lynch et al. (2017b)
ATCA	Aug 27 23:26:25 UTC	10	10.5	2.049	< 39	Lynch et al. (2017b)
e-MERLIN	Aug 28 12:00:00 UTC	11	5.0	0.512	< 90	Moldon et al. (2017a)
VLITE	Aug 30 23:10:28 UTC	13.45	0.3387	0.034	< 20400	Hallinan, Corsi et al. (2017)
LWA1	Aug 30 19:50:00 UTC	13	0.02585	0.016		Callister et al. (2017)
LWA1	Aug 30 19:50:00 UTC	13	0.04545	0.016		Callister et al. (2017)
VLA	Aug 30 22:09:24 UTC	13.41	10.0	-		K. Alexander et al. (2017)
e-MERLIN	Aug 31 13:00:00 UTC	14	5.0	0.512	< 109	Moldon et al. (2017b)
VLITE	Sep 1 20:44:59 UTC	15.37	0.3387	0.034	< 11400	Hallinan, Corsi et al. (2017)
ATCA	Sep 1 12:00:00 UTC	15	16.7	-	< 50	Troja et al. (2017c)
ATCA	Sep 1 12:00:00 UTC	15	21.2	-	< 50	Troja et al. (2017c)
ATCA	Sep 1 12:00:00 UTC	15	43.0	-	< 90	Troja et al. (2017c)
ATCA	Sep 1 12:00:00 UTC	15	45.0	-	< 90	Troja et al. (2017c)
e-MERLIN	Sep 1 13:00:00 UTC	15	5.0	0.512	< 114	Moldon et al. (2017b)
ALMA	Sep 1 20:22:05 UTC	15.33	97.5	-		K. Alexander et al. (2017)
VLA/JAGWAR	Sep 2 00:00:00 UTC	16	3.0		Detection	Mooley et al. (2017b)
e-MERLIN	Sep 2 13:00:00 UTC	16	5.0	0.512	144	Moldon et al. (2017b)
VLITE	Sep 2 18:51:34 UTC	16.36	0.3387	0.034	< 11700	Hallinan, Corsi et al. (2017)
e-MERLIN	Sep 3 13:00:00 UTC	17	5.0	0.512	< 166	Moldon et al. (2017b)
VLA	Sep 3 23:30:00 UTC	17	6.0		Detection	Corsi et al. (2017d)
VLITE	Sep 3 20:08:05 UTC	17.40	0.3387	0.034	< 6900	Hallinan, Corsi et al. (2017)
e-MERLIN	Sep 4 13:00:00 UTC	18	5.0	0.512	< 147	Moldon et al. (2017b)
ATCA	Sep 5 10:03:04 UTC	19	7.25		Detection	Murphy et al. (2017)
e-MERLIN	Sep 5 13:00:00 UTC	19	5.0	0.512	< 162	Moldon et al. (2017b)
VLA	Sep 5 22:12:00 UTC	19.47	6.0	-		Alexander et al. (2017d)
VLA	Sep 5 23:26:06 UTC	19.43	10.0	-		K. Alexander et al. (2017)
MeerKAT	Sep 6 03:22:00 UTC	20	1.48	0.22	<75	Goedhart et al. (2017a)

Table 5 continued

Table 5 *(continued)*

Telescope	UT date	Time since GW trigger (days)	Central frequency (GHz)	Bandwidth (GHz)	Flux (μ Jy), 3 σ	GCN/Reference
VLITE	Sep 7 19:09:43 UTC	21.36	0.3387	0.034	< 8100	Hallinan, Corsi et al. (2017)
SRT	Sep 7 10:41:00 UTC	20.92	7.2	0.68	< 1200	Aresu et al. (2017)
ATCA	Sep 8 12:00:00 UTC	22	17.0	-	< 35	Wieringa et al. (2017)
ATCA	Sep 8 12:00:00 UTC	22	21.0	-	< 35	Wieringa et al. (2017)
SRT	Sep 8 11:00:00 UTC	21.93	7.2	0.68	< 1500	Aresu et al. (2017)
VLITE	Sep 8 19:05:35 UTC	22.37	0.3387	0.034	<6300	Hallinan, Corsi et al. (2017)
SRT	Sep 9 10:37:00 UTC	22.92	7.2	0.68	< 1800	Aresu et al. (2017)
VLITE	Sep 9 18:52:45 UTC	23.36	0.3387	0.034	<4800	Hallinan, Corsi et al. (2017)
GMRT	Sep 9 11:30:00 UTC	23.0	1.39	0.032	–	Resmi et al. (2017); Kim et al. (2017)
e-MERLIN	Sep 10 13:00:00 UTC	24	5.0	0.512	< 126	Moldon et al. (2017b)
Effelsberg	Sep 10 13:10 UTC	24	5	2	< 30000	Kramer et al. (2017)
Effelsberg	Sep 10 13:35 UTC	24	32	2	< 90000	Kramer et al. (2017)
VLITE	Sep 10 18:36:48 UTC	24.35	0.3387	0.034	<6600	Hallinan, Corsi et al. (2017)
e-MERLIN	Sep 11 13:00:00 UTC	25	5.0	0.512	< 151	Moldon et al. (2017b)
e-MERLIN	Sep 12 13:00:00 UTC	26	5.0	0.512	< 113	Moldon et al. (2017b)
e-MERLIN	Sep 14 13:00:00 UTC	28	5.0	0.512	< 147	Moldon et al. (2017b)
e-MERLIN	Sep 15 13:00:00 UTC	29	5.0	0.512	< 106	Moldon et al. (2017b)
GMRT	Sep 16 07:30:00 UTC	29.8	1.39	0.032	–	Resmi et al. (2017); Kim et al. (2017)
e-MERLIN	Sep 16 13:00:00 UTC	30	5.0	0.512	< 118	Moldon et al. (2017b)
ALMA	Sep 16 20:36:21 UTC	30.34	97.5	-		K. Alexander et al. (2017)
MeerKAT	Sep 17 07:16:00 UTC	31	1.48	0.22	<60	Goedhart et al. (2017a)
e-MERLIN	Sep 17 13:00:00 UTC	31	5.0	0.512	<111	Moldon et al. (2017b)
e-MERLIN	Sep 18 13:00:00 UTC	32	5.0	0.512	111	Moldon et al. (2017b)
SRT	Sep 19 11:38:00 UTC	32.96	7.2	0.68	< 1200	Aresu et al. (2017)
EVN	Sep 20 10:00:00 UTC	34	5.0	0.256	< 84	Paragi et al. (2017b)
e-MERLIN	Sep 21 13:00:00 UTC	35	5.0	0.512	<132	Moldon et al. (2017b)
e-MERLIN	Sep 22 13:00:00 UTC	36	5.0	0.512	<121	Paragi et al. (2017b)
VLA	Sep 25 16:51:45 UTC	39.2	6.0 GHz		Detection	Alexander et al. 2017e

Table 6. Gamma-ray Coordinates Network (GCN) Notices and Circulars related to GW 170817 until Oct 1 2017 UTC

Telescope	UT date	Δt (days)	Obs. wavelength	References
Fermi/GBM	2017-08-17 12:41:20	0.0	gamma-ray	GCN Notice 524666471, Fermi-GBM (2017)
LIGO-Virgo/–	2017-08-17 13:21:42	0.03	gw	GCN 21505, The LIGO Scientific Collaboration et al. (2017a)
Fermi/GBM	2017-08-17 13:47:37	0.05	gamma-ray	GCN 21506, Connaughton et al. (2017)
INTEGRAL/SPI-ACS	2017-08-17 13:57:47	0.05	gamma-ray	GCN 21507, Savchenko et al. (2017a)
IceCube/–	2017-08-17 14:05:11	0.06	neutrino	GCN 21508, Bartos et al. (2017a)
LIGO-Virgo/–	2017-08-17 14:09:25	0.06	gw	GCN 21509, The LIGO Scientific Collaboration et al. (2017f)
LIGO-Virgo/–	2017-08-17 14:38:46	0.08	gw	GCN 21510, The LIGO Scientific Collaboration et al. (2017g)
IceCube/–	2017-08-17 14:54:58	0.09	neutrino	GCN 21511, Bartos et al. (2017c)
LIGO-Virgo/–	2017-08-17 17:54:51	0.22	gw	GCN 21513, The LIGO Scientific Collaboration et al. (2017b)
Astrosat/CZTI	2017-08-17 18:16:42	0.23	gamma-ray	GCN 21514, Balasubramanian et al. (2017)
IPN/–	2017-08-17 18:35:12	0.25	gamma-ray	GCN 21515, Svinkin et al. (2017b)
–/–	2017-08-17 18:55:12	0.26		GCN 21516, Dálya et al. (2017)
Insight-HXMT/HE	2017-08-17 19:35:28	0.29	gamma-ray	GCN 21518, Liao et al. (2017)

Table 6 continued

Table 6 *(continued)*

Telescope	UT date	Δt (days)	Obs. wavelength	References
–/–	2017-08-17 20:00:07	0.3		GCN 21519, Cook et al. (2017a)
Fermi/GBM	2017-08-17 20:00:07	0.3	gamma-ray	GCN 21520, von Kienlin et al. (2017)
–/–	2017-08-17 20:12:41	0.31		GCN 21521, Cook et al. (2017b)
ANTARES/–	2017-08-17 20:35:31	0.33	neutrino	GCN 21522, Ageron et al. (2017a)
Swift/BAT	2017-08-17 21:34:36	0.37	gamma-ray	GCN 21524, Barthelmy et al. (2017)
AGILE/MCAL	2017-08-17 22:01:26	0.39	gamma-ray	GCN 21525, Pilia et al. (2017)
AGILE/GRID	2017-08-17 22:22:43	0.4	gamma-ray	GCN 21526, Piano et al. (2017)
LIGO-Virgo/–	2017-08-17 23:54:40	0.47	gw	GCN 21527, The LIGO Scientific Collaboration et al. (2017c)
Fermi/GBM	2017-08-18 00:36:12	0.5	gamma-ray	GCN 21528, Goldstein et al. (2017)
Swope/–	2017-08-18 01:05:23	0.52	optical	GCN 21529, Coulter et al. (2017a)
DECam/–	2017-08-18 01:15:01	0.52	optical	GCN 21530, Allam et al. (2017)
DLT40/–	2017-08-18 01:41:13	0.54	optical	GCN 21531, Yang et al. (2017a)
REM-ROS2/–	2017-08-18 02:00:40	0.56	optical, IR	GCN 21532, Melandri et al. (2017a)
ASAS-SN/–	2017-08-18 02:06:30	0.56	optical	GCN 21533, Cowperthwaite et al. (2017b)
Fermi/LAT	2017-08-18 02:09:53	0.56	gamma-ray	GCN 21534, Kocevski et al. (2017)
–/–	2017-08-18 02:48:50	0.59		GCN 21535, Cook et al. (2017c)
HST/–	2017-08-18 03:01:20	0.6	optical	GCN 21536, Foley et al. (2017a)
ATCA/–	2017-08-18 04:04:00	0.64	radio	GCN 21537, Bannister et al. (2017c)
LasCumbres/–	2017-08-18 04:06:31	0.64	optical	GCN 21538, Arcavi et al. (2017a)
DLT40/–	2017-08-18 04:11:35	0.65	optical	GCN 21539, Yang et al. (2017c)
DECam/–	2017-08-18 04:44:32	0.67	optical	GCN 21541, Nicholl et al. (2017a)
SkyMapper/–	2017-08-18 04:46:27	0.67	optical	GCN 21542, Moller et al. (2017)
LasCumbres/–	2017-08-18 04:54:23	0.68	optical	GCN 21543, Arcavi et al. (2017d)
VISTA/VIRCAM	2017-08-18 05:03:48	0.68	optical, IR	GCN 21544, Tanvir et al. (2017a)
VLA/–	2017-08-18 05:07:58	0.69	radio	GCN 21545, Alexander et al. (2017a)
MASTER/–	2017-08-18 05:37:59	0.71	optical	GCN 21546, Lipunov et al. (2017a)
Magellan/–	2017-08-18 05:46:33	0.71	optical	GCN 21547, Drout et al. (2017)
VLA/–	2017-08-18 06:56:44	0.76	radio	GCN 21548, Alexander et al. (2017b)
Subaru/HSC	2017-08-18 07:07:07	0.77	optical	GCN 21549, Yoshida et al. (2017a)
Swift/UVOT,XRT	2017-08-18 07:24:04	0.78	x-ray, uv	GCN 21550, Evans et al. (2017)
Magellan/LDSS-3	2017-08-18 07:54:23	0.8	optical	GCN 21551, Simon et al. (2017)
Gemini-South/Flamingos-2	2017-08-18 08:00:58	0.81	IR	GCN 21552, Singer et al. (2017a)
Pan-STARRS/–	2017-08-18 08:37:20	0.83	optical	GCN 21553, Chambers et al. (2017a)
HCT/HFOSC	2017-08-18 09:54:21	0.88	optical	GCN 21554, Pavana et al. (2017)
MAXI/GSC/–	2017-08-18 10:43:45	0.92	x-ray	GCN 21555, Sugita et al. (2017)
REM-ROS2/–	2017-08-18 10:54:42	0.93	optical	GCN 21556, Melandri et al. (2017b)
–/–	2017-08-18 12:15:23	0.98		GCN 21557, Foley et al. (2017b)
TZAC/TAROT-Reunion	2017-08-18 13:04:25	1.02	optical	GCN 21558, Klotz et al. (2017)
ATCA/–	2017-08-18 13:27:25	1.03	radio	GCN 21559, Bannister et al. (2017a)
SkyMapper/–	2017-08-18 13:54:11	1.05	optical	GCN 21560, Wolf et al. (2017)
Subaru/HSC	2017-08-18 14:27:26	1.07	optical	GCN 21561, Yoshida et al. (2017b)
ASKAP/–	2017-08-18 14:36:00	1.08	radio	GCN 21562, Bannister et al. (2017d)
LSGT,T17/SNUCAM-II	2017-08-18 14:45:33	1.09	optical	GCN 21563, Im et al. (2017a)
AGILE/GRID	2017-08-18 15:22:43	1.11	gamma-ray	GCN 21564, Bulgarelli et al. (2017)
LasCumbres/–	2017-08-18 15:58:41	1.14	optical	GCN 21565, Arcavi et al. (2017b)
LSGT,T17/SNUCAM-II	2017-08-18 17:15:43	1.19	optical	GCN 21566, Im et al. (2017b)
Swope/–	2017-08-18 17:19:22	1.19	optical	GCN 21567, Coulter et al. (2017b)
IceCube/–	2017-08-18 17:27:25	1.2	neutrino	GCN 21568, Bartos et al. (2017b)
Gemini-South/–	2017-08-18 17:44:26	1.21	optical, IR	GCN 21569, Singer et al. (2017c)

Table 6 continued

Table 6 *(continued)*

Telescope	UT date	Δt (days)	Obs. wavelength	References
MASTER/–	2017-08-18 18:06:51	1.23	optical	GCN 21570, Lipunov et al. (2017b)
VLA/–	2017-08-18 18:16:30	1.23	radio	GCN 21571, Williams et al. (2017b)
Swift/UVOT,XRT	2017-08-18 18:32:37	1.24	x-ray, uv	GCN 21572, Cenko et al. (2017)
ATCA/–	2017-08-18 20:19:00	1.32	radio	GCN 21574, Kaplan et al. (2017a)
2MASS,Spitzer/–	2017-08-18 20:23:05	1.32	IR	GCN 21575, Eikenberry et al. (2017)
VISTA/VIRCam	2017-08-18 21:16:32	1.36	IR	GCN 21576, Tanvir et al. (2017b)
–/–	2017-08-18 23:00:31	1.43		GCN 21577, Malesani et al. (2017b)
–/–	2017-08-18 23:11:30	1.44		GCN 21578, Cowperthwaite et al. (2017a)
PROMPT5/–	2017-08-19 00:18:04	1.48	optical	GCN 21579, Yang et al. (2017b)
DECam/–	2017-08-19 00:22:23	1.49	optical	GCN 21580, Nicholl et al. (2017b)
LasCumbres/–	2017-08-19 01:26:07	1.53	optical	GCN 21581, Arcavi et al. (2017c)
NTT/–	2017-08-19 01:46:26	1.55	optical, IR	GCN 21582, Lyman et al. (2017)
Swope/–	2017-08-19 01:54:36	1.55	optical	GCN 21583, Kilpatrick et al. (2017)
GROND/–	2017-08-19 01:58:14	1.55	optical, IR	GCN 21584, Wiseman et al. (2017)
SOAR/GoodmanSpectrograph	2017-08-19 03:10:19	1.6	IR, optical	GCN 21585, Nicholl et al. (2017c)
Subaru/HSC	2017-08-19 06:52:33	1.76	optical	GCN 21586, Yoshida et al. (2017c)
MASTER/–	2017-08-19 08:10:30	1.81	optical	GCN 21587, V.M.Lipunov et al. (2017b)
VLBA/–	2017-08-19 09:36:26	1.87	radio	GCN 21588, Deller et al. (2017a)
VLA/–	2017-08-19 09:51:33	1.88	radio	GCN 21589, Alexander et al. (2017c)
Pan-STARRS/–	2017-08-19 10:14:53	1.9	optical	GCN 21590, Chambers et al. (2017b)
NOT/NOTCam	2017-08-19 12:00:05	1.97	IR	GCN 21591, Malesani et al. (2017a)
ESO-VLT/X-shooter	2017-08-19 12:16:37	1.98	IR, optical	GCN 21592, Pian et al. (2017)
ESO-VLT/FORS2	2017-08-19 14:13:15	2.06	optical	GCN 21594, Wiersema et al. (2017)
Subaru/HSC	2017-08-19 14:46:41	2.09	optical	GCN 21595, Tominaga et al. (2017)
REM-ROS2/–	2017-08-19 16:38:19	2.16	optical	GCN 21596, Melandri et al. (2017c)
KMTNet/wide-fieldcamera	2017-08-19 16:55:08	2.18	optical	GCN 21597, Im et al. (2017d)
ESO-VST/OmegaCam	2017-08-19 17:37:19	2.21	optical	GCN 21598, Grado et al. (2017c)
LaSilla-QUEST/–	2017-08-19 18:04:05	2.22	optical	GCN 21599, Rabinowitz et al. (2017)
GMRT/–	2017-08-19 21:18:21	2.36	radio	GCN 21603, De et al. (2017a)
PROMPT5/–	2017-08-19 23:31:25	2.45	optical	GCN 21606, Valenti et al. (2017)
GROND/–	2017-08-20 04:49:21	2.67	optical, IR	GCN 21608, Chen et al. (2017)
VIRT/–	2017-08-20 05:27:49	2.7	optical	GCN 21609, Gendre et al. (2017)
SALT/–	2017-08-20 06:14:37	2.73	optical	GCN 21610, Shara et al. (2017)
Swift/XRT	2017-08-20 08:42:40	2.83	x-ray	GCN 21612, Evans et al. (2017)
VLA/–	2017-08-20 09:17:57	2.86	radio	GCN 21613, Corsi et al. (2017b)
VLA/–	2017-08-20 10:26:01	2.91	radio	GCN 21614, Corsi et al. (2017a)
Pan-STARRS/–	2017-08-20 13:59:50	3.05	optical	GCN 21617, Chambers et al. (2017c)
ChilescopeRC-1000/–	2017-08-20 14:24:47	3.07	optical	GCN 21618, Pozanenko et al. (2017d)
TOROS/–	2017-08-20 14:48:49	3.09	optical	GCN 21619, Diaz et al. (2017a)
TOROS/–	2017-08-20 15:03:42	3.1	optical	GCN 21620, Diaz et al. (2017c)
–/–	2017-08-20 15:40:35	3.12		GCN 21621, V.M.Lipunov (2017)
Kanata/HONIR	2017-08-20 16:37:38	3.16	IR	GCN 21623, Nakaoka et al. (2017)
BOOTES-5/–	2017-08-20 21:59:59	3.39	optical	GCN 21624, Castro-Tirado et al. (2017)
ASKAP/–	2017-08-21 00:58:33	3.51	radio	GCN 21625, Dobie et al. (2017b)
NuSTAR/–	2017-08-21 04:33:27	3.66	x-ray	GCN 21626, Harrison et al. (2017)
Zadko/–	2017-08-21 05:57:23	3.72	optical	GCN 21627, Coward et al. (2017b)
ATCA/–	2017-08-21 07:45:30	3.79	radio	GCN 21628, Lynch et al. (2017c)
ATCA/–	2017-08-21 09:02:12	3.85	radio	GCN 21629, Lynch et al. (2017d)
ANTARES/–	2017-08-21 15:08:00	4.1	neutrino	GCN 21631, Ageron et al. (2017b)
KMTNet,iTelescope.NET/–	2017-08-21 15:49:41	4.13	optical	GCN 21632, Im et al. (2017c)

Table 6 continued

Table 6 *(continued)*

Telescope	UT date	Δt (days)	Obs. wavelength	References
Pan-STARRS/–	2017-08-21 16:03:52	4.14	optical	GCN 21633, Chambers et al. (2017d)
TOROS/CASLEO	2017-08-21 16:05:22	4.14	optical	GCN 21634, Diaz et al. (2017d)
ChilescopeRC-1000/–	2017-08-21 16:11:53	4.15	optical	GCN 21635, Pozanenko et al. (2017a)
VLA/–	2017-08-21 18:40:08	4.25	radio	GCN 21636, Corsi et al. (2017e)
MWA/–	2017-08-22 00:59:36	4.51	radio	GCN 21637, Kaplan et al. (2017c)
Gemini-South/Flamingos-2	2017-08-22 05:20:11	4.69	IR	GCN 21638, Chornock et al. (2017b)
ASKAP/–	2017-08-22 07:23:04	4.78	radio	GCN 21639, Dobie et al. (2017a)
CALET/CGBM	2017-08-22 09:36:51	4.87	gamma-ray	GCN 21641, Nakahira et al. (2017)
ChilescopeRC-1000/–	2017-08-22 15:23:04	5.11	optical	GCN 21644, Pozanenko et al. (2017c)
6dFGS/–	2017-08-22 16:55:17	5.18	optical	GCN 21645, Sadler et al. (2017)
Chandra/CXO	2017-08-22 18:06:23	5.23	x-ray	GCN 21648, Margutti et al. (2017)
VLA/JAGWAR	2017-08-22 19:13:38	5.27	radio	GCN 21650, Mooley et al. (2017a)
ESO-VLT/FORS2	2017-08-23 07:52:38	5.8	optical	GCN 21653, D'Avanzo et al. (2017)
VLA/–	2017-08-23 18:25:07	6.24	radio	GCN 21664, Corsi et al. (2017c)
HST/Pan-STARRS1/–	2017-08-24 01:39:20	6.54	optical	GCN 21669, Yu et al. (2017)
ATCA/–	2017-08-24 04:30:05	6.66	radio	GCN 21670, Lynch et al. (2017a)
ASKAP/–	2017-08-24 06:10:24	6.73	radio	GCN 21671, Bannister et al. (2017b)
INTEGRAL/SPI,IBIS,JEM-X,OMC	2017-08-24 09:03:02	6.85	gamma-ray, x-ray, optical	GCN 21672, Savchenko et al. (2017b)
H.E.S.S./–	2017-08-24 10:35:02	6.91	gamma-ray	GCN 21674, de Naurois et al. (2017)
LOFAR/ILT	2017-08-24 13:35:06	7.04	radio	GCN 21676, Broderick et al. (2017)
AAT/AAO	2017-08-24 15:31:25	7.12	optical	GCN 21677, Andreoni et al. (2017)
LWA/LWA1	2017-08-24 16:08:17	7.14	radio	GCN 21680, Callister et al. (2017a)
ESO-VLT/MUSEIntegralFieldUnit	2017-08-24 19:28:30	7.28	optical	GCN 21681, Levan et al. (2017b)
Gemini-South/Flamingos-2,GMOS	2017-08-24 19:31:19	7.28	optical, IR	GCN 21682, Troja et al. (2017a)
HAWC/–	2017-08-24 19:35:19	7.29	gamma-ray	GCN 21683, Martinez-Castellanos et al. (2017)
Gemini-South/Flamingos-2	2017-08-25 04:04:17	7.64	IR	GCN 21684, Chornock et al. (2017a)
Subaru/HSC	2017-08-25 07:38:17	7.79	optical	GCN 21685, Yoshida et al. (2017d)
Auger/SurfaceDetector	2017-08-25 08:13:23	7.81	neutrino	GCN 21686, Alvarez-Muniz et al. (2017)
MASTER/MASTER-II	2017-08-25 08:48:24	7.84	optical	GCN 21687, V.M.Lipunov et al. (2017a)
ESO-VST/OmegaCAM	2017-08-25 22:15:33	8.4	optical	GCN 21703, Grado et al. (2017a)
GMRT/–	2017-08-26 01:23:58	8.53	radio	GCN 21708, De et al. (2017b)
ATCA/–	2017-08-29 03:49:22	11.63	radio	GCN 21740, Lynch et al. (2017b)
Zadko/–	2017-08-29 08:29:39	11.83	optical	GCN 21744, Coward et al. (2017a)
Konus-Wind/–	2017-08-29 10:55:08	11.93	gamma-ray	GCN 21746, Svinkin et al. (2017a)
ALMA/–	2017-08-29 12:37:56	12.0	radio	GCN 21747, Schulze et al. (2017)
ALMA/–	2017-08-29 14:55:15	12.09	radio	GCN 21750, Williams et al. (2017a)
OVRO/–	2017-08-30 03:23:28	12.61	radio	GCN 21760, Pearson et al. (2017)
EVN/VLBI	2017-08-30 09:48:26	12.88	radio	GCN 21763, Paragi et al. (2017a)
Chandra/CXO	2017-08-30 12:07:12	12.98	x ray	GCN 21765, Troja et al. (2017a)
GMRT/–	2017-08-30 16:06:24	13.14	radio	GCN 21768, Resmi et al. (2017)
Gemini-South/–	2017-08-31 18:28:50	14.24	IR	GCN 21778, Troja et al. (2017b)
Gemini-South/Flamingos-2	2017-08-31 18:32:01	14.24	IR	GCN 21779, Singer et al. (2017b)
HST/–	2017-08-31 20:33:24	14.33	optical, IR	GCN 21781, Levan et al. (2017a)
PioftheSky/PioftheSkyNorth	2017-09-01 21:54:25	15.38	optical	GCN 21783, Cwiek et al. (2017)
AGILE/GRID	2017-09-02 16:54:59	16.18	gamma-ray	GCN 21785, Verrecchia et al. (2017)
Chandra/CXO	2017-09-02 16:57:54	16.18	x ray	GCN 21786, Fong et al. (2017)
Chandra/CXO	2017-09-02 17:06:21	16.18	x ray	GCN 21787, Troja et al. (2017b)
Chandra/CXO	2017-09-03 20:24:16	17.32	x ray	GCN 21798, Haggard et al. (2017b)
ATCA/–	2017-09-04 02:26:14	17.57	radio	GCN 21803, Troja et al. (2017c)
e-MERLIN/–	2017-09-04 07:48:43	17.8	radio	GCN 21804, Moldon et al. (2017a)

Table 6 continued

Table 6 *(continued)*

Telescope	UT date	Δt (days)	Obs. wavelength	References
VLA/–	2017-09-04 22:14:55	18.4	radio	GCN 21814, Mooley et al. (2017b)
VLA/–	2017-09-04 22:14:59	18.4	radio	GCN 21815, Corsi et al. (2017d)
HST/HST,Gaia	2017-09-05 00:30:09	18.49	optical, IR, uv	GCN 21816, Adams et al. (2017)
ESO-VST/OMEGACam	2017-09-06 15:07:27	20.1	optical	GCN 21833, Grado et al. (2017b)
ATCA/–	2017-09-07 02:31:55	20.58	radio	GCN 21842, Murphy et al. (2017)
LWA/LWA1	2017-09-08 02:47:01	21.59	radio	GCN 21848, Callister et al. (2017b)
VLBA/–	2017-09-08 11:16:27	21.94	radio	GCN 21850, Deller et al. (2017b)
VLA/–	2017-09-08 13:23:16	22.03	radio	GCN 21851, Alexander et al. (2017d)
ATCA/–	2017-09-14 05:25:42	27.7	radio	GCN 21882, Wieringa et al. (2017)
AST3-2/–	2017-09-15 03:45:21	28.63	optical	GCN 21883, Hu et al. (2017)
ATLAS/–	2017-09-15 11:24:15	28.95	optical	GCN 21886, Tonry et al. (2017)
DanishTel/–	2017-09-15 16:40:07	29.17	optical	GCN 21889, Cano et al. (2017)
MeerKAT/–	2017-09-15 20:16:29	29.32	radio	GCN 21891, Goedhart et al. (2017b)
DFN/–	2017-09-18 13:45:29	32.04	optical	GCN 21894, Hancock et al. (2017)
T80S,EABA/–	2017-09-18 16:22:27	32.15	optical	GCN 21895, Diaz et al. (2017b)
VLBA/–	2017-09-19 07:51:22	32.8	radio	GCN 21897, Deller et al. (2017c)
ChilescopeRC-1000/–	2017-09-19 18:09:03	33.23	optical	GCN 21898, Pozanenko et al. (2017b)
Parkes/–	2017-09-21 02:38:29	34.58	radio	GCN 21899, Bailes et al. (2017a)
ATCA/–	2017-09-21 06:42:36	34.75	radio	GCN 21900, Ricci et al. (2017)
LasCumbres/FLOYDS,Gemini	2017-09-22 03:24:44	35.61	optical	GCN 21908, McCully et al. (2017)
SRT/–	2017-09-22 19:06:44	36.27	radio	GCN 21914, Aresu et al. (2017)
Effelsberg/–	2017-09-23 20:34:41	37.33	radio	GCN 21920, Kramer et al. (2017)
MWA/–	2017-09-25 22:30:34	39.41	radio	GCN 21927, Kaplan et al. (2017b)
Parkes/–	2017-09-26 02:00:59	39.56	radio	GCN 21928, Bailes et al. (2017b)
VLA/–	2017-09-26 05:14:16	39.69	radio	GCN 21929, Hallinan et al. (2017)
PioftheSky/PioftheSkyNorth	2017-09-26 21:17:49	40.36	optical	GCN 21931, Batsch et al. (2017)
MeerKAT/–	2017-09-27 13:19:14	41.03	radio	GCN 21933, Goedhart et al. (2017a)
VLA/–	2017-09-27 19:03:46	41.27	radio	GCN 21935, Alexander et al. (2017e)
EVN/–	2017-09-28 10:35:27	41.91	radio	GCN 21939, Paragi et al. (2017b)
e-MERLIN/–	2017-09-28 11:12:37	41.94	radio	GCN 21940, Moldon et al. (2017b)

REFERENCES

????

Aab, A., et al. 2015a, Nucl. Instrum. Methods Phys. Res. Sect. A, 798, 172

—. 2015b, Phys. Rev. D, 91, 092008

Aartsen, M., et al. 2016, Journal of Instrumentation, 11, P11009

Aartsen, M. G., Ackermann, M., Adams, J., et al. 2015, PhRvD, 91, 022001

—. 2017, Journal of Instrumentation, 12, P03012

Abadie, J., Abbott, B. P., Abbott, R., et al. 2010, Classical and Quantum Gravity, 27, 173001

Abbott, B. P., et al. 2016a, PhRvL, 116, 061102

—. 2016b, PhRvL, 116, 241103

Abbott, B. P., Abbott, R., Abbott, T. D., et al. 2016, ApJL, 826, L13

Abbott, B. P., et al. 2016, PhRvL, 116, 241102

—. 2017a, PhRvL, 118, 221101

—. 2017b, PhRvL, 118, 221101

—. 2017c, PhRvL, 119, 161101

Abdalla, H. et al. (H.E.S.S. Collaboration). 2017

Abeysekara, A. U., Albert, A., Alfaro, R., et al. 2017, ApJ, 843, 39

Adams, S. M., et al. 2017, GCN, 21816, 1

Ade, P. A. R., et al. 2016, A&A, 594, A13

Ageron, M., et al. 2011, Nucl. Instr. Meth. Phys. Res. A, 656, 11

—. 2017a, GCN, 21522, 1

—. 2017b, GCN, 21631, 1

Alexander, K., et al. 2017a, GCN, 21545, 1

—. 2017b, GCN, 21548, 1

—. 2017c, GCN, 21589, 1

Alexander, K. D., et al. 2017d, GCN, 21851, 1

—. 2017e, GCN, 21935, 1

Allam, S., et al. 2017, GCN, 21530, 1

Allen, B., Anderson, W. G., Brady, P. R., Brown, D. A., & Creighton, J. D. E. 2012, PhRvD, 85, 122006

Alvarez-Muniz, J., et al. 2017, GCN, 21686, 1

Andreoni, I., et al. 2017, GCN, 21677, 1

Arcavi, I., et al. 2017a, GCN, 21538, 1
—. 2017b, GCN, 21565, 1
—. 2017c, GCN, 21581, 1
—. 2017d, GCN, 21543, 1
Arcavi et al. 2017a, ApJL, ApJL in preparation
—. 2017b, Nature, Nature in press
Aresu, G., et al. 2017, GCN, 21914, 1
Baade, W., & Zwicky, F. 1934, Physical Review, 46, 76
Bagot, P., Portegies Zwart, S. F., & Yungelson, L. R. 1998, A&A, 332, L57
Bailes, M., et al. 2017a, GCN, 21899, 1
—. 2017b, GCN, 21928, 1
Baker, J. G., et al. 2006, 96, 111102
Balasubramanian, A., et al. 2017, GCN, 21514, 1
Bannister, K., et al. 2017a, GCN, 21559, 1
—. 2017b, GCN, 21671, 1
—. 2017c, GCN, 21537, 1
—. 2017d, GCN, 21562, 1
Bannister, K. W., Shannon, R. M., Macquart, J.-P., et al. 2017, ApJL, 841, L12
Barnes, J., & Kasen, D. 2013, ApJ, 775, 18
Barnes, J., Kasen, D., Wu, M.-R., & Mart'inez-Pinedo, G. 2016, ArXiv e-prints, arXiv:1605.07218
Barr, E. D., Guillemot, L., Champion, D. J., et al. 2013, MNRAS, 429, 1633
Barthelmy, S. D., Chincarini, G., Burrows, D. N., et al. 2005, Nature, 438, 994
Barthelmy, S. D., et al. 2017, GCN, 21524, 1
Bartos, I., et al. 2017a, GCN, 21508, 1
—. 2017b, GCN, 21568, 1
—. 2017c, GCN, 21511, 1
Batsch, T., et al. 2017, GCN, 21931, 1
Belczynski, K., Kalogera, V., & Bulik, T. 2002, ApJ, 572, 407
Berger, E. 2010, ApJ, 722, 1946
—. 2014, ARA&A, 52, 43
Berger, E., Fong, W., & Chornock, R. 2013a, ApJL, 774, L23
—. 2013b, ApJL, 774, L23
Berger, E., Price, P. A., Cenko, S. B., et al. 2005, Nature, 438, 988
Berger, E., Fox, D. B., Price, P. A., et al. 2007, ApJ, 664, 1000
Bhalerao, V., Bhattacharya, D., Vibhute, A., et al. 2017, Journal of Astrophysics and Astronomy, 38, 31. https://doi.org/10.1007/s12036-017-9447-8
Blackburn, L., Briggs, M. S., Camp, J., et al. 2015, ApJS, 217, 8
Blanchet, L. 2014, Living Rev. Rel., 17, 2
Blanchet, L., Buonanno, A., & Faye, G. 2006, PhRvD, 74, 104034, [Erratum: PhRvD **75**, 049903 (2007), Erratum: PhRvD **81**, 089901 (2010),]
Blanchet, L., et al. 1995, PhRvL, 74, 3515
—. 2004, PhRvL, 93, 091101
Bloom, J. S., Sigurdsson, S., & Pols, O. R. 1999, MNRAS, 305, 763
Bohé, A., Marsat, S., & Blanchet, L. 2013, Class. Quant. Grav., 30, 135009
Broderick, J., et al. 2017, GCN, 21676, 1
Brown, T. M., Baliber, N., Bianco, F. B., et al. 2013, PASP, 125, 1031
Buckley et al. 2017, MNRAS letters, submitted
Bulgarelli, A., et al. 2017, GCN, 21564, 1
Buonanno, A., & Damour, T. 1999, 59, 084006
Burrows, D. N., Hill, J. E., Nousek, J. A., et al. 2005, SSRv, 120, 165
Burrows, D. N., Grupe, D., Capalbi, M., et al. 2006, ApJ, 653, 468
Callister, T., et al. 2017a, GCN, 21680, 1
—. 2017b, GCN, 21848, 1
Campanelli, M., et al. 2006, 96, 111101
Cannon, K., et al. 2012, ApJ, 748, 136
Cano, Z., et al. 2017, GCN, 21889, 1
Castro-Tirado, A. J., et al. 2017, GCN, 21624, 1
Cenko, S. B., et al. 2017, GCN, 21572, 1
Chambers, K. C., Magnier, E. A., Metcalfe, N., et al. 2016, ArXiv e-prints, arXiv:1612.05560
Chambers, K. C., et al. 2017a, GCN, 21553, 1
—. 2017b, GCN, 21590, 1
—. 2017c, GCN, 21617, 1
—. 2017d, GCN, 21633, 1
Chen, T.-W., et al. 2017, GCN, 21608, 1
Chornock, R., et al. 2017a, GCN, 21684, 1
—. 2017b, GCN, 21638, 1
Clark, J. P. A. 1979, in Sources of Gravitational Radiation, ed. L. L. Smarr, 447–459
Clark, J. P. A., van den Heuvel, E. P. J., & Sutantyo, W. 1979, A&A, 72, 120
Clarke, T. E., Kassim, N. E., Brisken, W., et al. 2016, in Proc. SPIE, Vol. 9906, Ground-based and Airborne Telescopes VI, 99065B
Connaughton, V., et al. 2017, GCN, 21506, 1
Cook, D., & Kasliwal, M. 2017, to be submitted
Cook, D. O., et al. 2017a, GCN, 21519, 1
—. 2017b, GCN, 21521, 1
—. 2017c, GCN, 21535, 1
Corsi, A., et al. 2017a, GCN, 21614, 1
—. 2017b, GCN, 21613, 1
—. 2017c, GCN, 21664, 1
—. 2017d, GCN, 21815, 1
—. 2017e, GCN, 21636, 1
Coulter, D. A., et al. 2017a, GCN, 21529, 1
—. 2017b, GCN, 21567, 1
Coulter et al. 2017, Science, doi:10.1126/science.aap9811

Covino, S., Wiersema, K., Fan, Y., & Toma, K. 2017, Nature in press, doi:10.1038/s41550-017-0285-z
Coward, D., et al. 2017a, GCN, 21744, 1
—. 2017b, GCN, 21627, 1
Cowperthwaite, P., et al. 2017a, GCN, 21578, 1
Cowperthwaite, P. S., et al. 2017b, GCN, 21533, 1
Cutler, C., et al. 1993, PhRvL, 70, 2984
Cwiek, A., et al. 2017, GCN, 21783, 1
Dalya, G., Frei, Z., Galgoczi, G., Raffai, P., & de Souza, R. 2016, VizieR Online Data Catalog, 7275
Dalya, G., Frei, Z., Galgoczi, G., Raffai, P., & de Souza, R. S. 2016, VizieR Online Data Catalog, 7275
Dálya, G., et al. 2017, GCN, 21516, 1
Damour, T., & Taylor, J. H. 1991, ApJ, 366, 501
—. 1992, PhRvD, 45, 1840
D'Avanzo, P., Malesani, D., Covino, S., et al. 2009, A&A, 498, 711
D'Avanzo, P., et al. 2017, GCN, 21653, 1
De, K., et al. 2017a, GCN, 21603, 1
—. 2017b, GCN, 21708, 1
de Naurois, M., et al. 2017, GCN, 21674, 1
Deller, A., et al. 2017a, GCN, 21588, 1
—. 2017b, GCN, 21850, 1
—. 2017c, GCN, 21897, 1
Dewey, R. J., & Cordes, J. M. 1987, ApJ, 321, 780
Dezalay, J.-P., Barat, C., Talon, R., et al. 1992, in American Institute of Physics Conference Series, Vol. 265, American Institute of Physics Conference Series, ed. W. S. Paciesas & G. J. Fishman, 304–309
Diaz, M., et al. 2017a, GCN, 21619, 1
—. 2017b, GCN, 21895, 1
—. 2017c, GCN, 21620, 1
—. 2017d, GCN, 21634, 1
Dobie, D., et al. 2017a, GCN, 21639, 1
—. 2017b, GCN, 21625, 1
Drout, M. R., et al. 2017, GCN, 21547, 1
Drout et al. 2017, Science, doi:10.1126/science.aaq0049
Eichler, D., Livio, M., Piran, T., & Schramm, D. N. 1989, Nature, 340, 126
Eikenberry, S., et al. 2017, GCN, 21575, 1
Einstein, A. 1916, Sitzungsberichte der Königlich Preußischen Akademie der Wissenschaften (Berlin), 1, 688
—. 1918, Sitzungsberichte der Königlich Preußischen Akademie der Wissenschaften (Berlin), 1, 154
Ellingson, S. W., Taylor, G. B., Craig, J., et al. 2013, IEEE Transactions on Antennas and Propagation, 61, 2540
Evans, P., et al. 2017, GCN, 21550, 1
Evans, P., Cenko, S., Kennea, J. A., et al. 2017, doi:10.1126/science.aap9580, science, submitted
Evans, P., et al. 2017, GCN, 21612, 1
Fermi-GBM. 2017, GCN, 524666471, 1. https://gcn.gsfc.nasa.gov/other/524666471.fermi
Feroci, M., Costa, E., Soffitta, P., et al. 2007, Nuclear Instruments and Methods in Physics Research A, 581, 728
Fixsen, D. J. 2009, Astrophys. J., 707, 916
Flannery, B. P., & van den Heuvel, E. P. J. 1975, A&A, 39, 61
Flaugher, B., Diehl, H. T., Honscheid, K., et al. 2015, AJ, 150, 150
Foley, R. J., et al. 2017a, GCN, 21536, 1
—. 2017b, GCN, 21557, 1
Fong, W., & Berger, E. 2013, ApJ, 776, 18
Fong, W., Berger, E., Margutti, R., & Zauderer, B. A. 2015, ApJ, 815, 102
Fong, W., Berger, E., Chornock, R., et al. 2013, ApJ, 769, 56
Fong, W., et al. 2017, GCN, 21786, 1
Fox, D. B., Frail, D. A., Price, P. A., et al. 2005a, Nature, 437, 845
—. 2005b, Nature, 437, 845
Freedman, W. L., Madore, B. F., Gibson, B. K., et al. 2001, ApJ, 553, 47
Fryer, C. L., Woosley, S. E., & Hartmann, D. H. 1999, ApJ, 526, 152
Gehrels, N. 2004, in American Institute of Physics Conference Series, Vol. 727, Gamma-Ray Bursts: 30 Years of Discovery, ed. E. Fenimore & M. Galassi, 637–641
Gehrels, N., Cannizzo, J. K., Kanner, J., et al. 2016, ApJ, 820, 136
Gehrels, N., Sarazin, C. L., O'Brien, P. T., et al. 2005, Nature, 437, 851
Gendre, B., et al. 2017, GCN, 21609, 1
Giacconi, R., Gursky, H., Paolini, F. R., & Rossi, B. B. 1962, Phys. Rev. Lett., 9, 439
Goedhart, S., et al. 2017a, GCN, 21933, 1
—. 2017b, GCN, 21891, 1
Gold, T. 1968, Nature, 218, 731
—. 1969, Nature, 221, 25
Goldstein, A., Burgess, J. M., Preece, R. D., et al. 2012, ApJS, 199, 19
Goldstein, A., et al. 2017, ApJL, 848, doi:10.3847/2041-8213/aa8f41
Goldstein, A., et al. 2017, GCN, 21528, 1
Goodman, J. 1986, ApJL, 308, L47
Gottlieb, O., Nakar, E., & Piran, T. 2017, ArXiv e-prints, arXiv:1705.10797
Grado, A., et al. 2017a, GCN, 21703, 1
—. 2017b, GCN, 21833, 1
—. 2017c, GCN, 21598, 1
Grossman, D., Korobkin, O., Rosswog, S., & Piran, T. 2014, MNRAS, 439, 757
Gruber, D., Goldstein, A., Weller von Ahlefeld, V., et al. 2014, ApJS, 211, 12
Haggard, D., Nynka, M., Ruan, J. J., et al. 2017a, doi:10.3847/2041-8213/aa8ede, apJLetters, in press

Haggard, D., et al. 2017b, GCN, 21798, 1
Hallinan, G., et al. 2017, GCN, 21929, 1
Hallinan, Corsi et al. 2017, *submitted*
Hancock, P. J., et al. 2017, GCN, 21894, 1
Harrison, F. A., Craig, W. W., Christensen, F. E., et al. 2013, ApJ, 770, 103
Harrison, F. A., et al. 2017, GCN, 21626, 1
Hewish, A., Bell, S. J., Pilkington, J. D. H., Scott, P. F., & Collins, R. A. 1968, Nature, 217, 709
Hjorth, J., Watson, D., Fynbo, J. P. U., et al. 2005a, Nature, 437, 859
—. 2005b, Nature, 437, 859
Hjorth, J., Sollerman, J., Gorosabel, J., et al. 2005c, ApJL, 630, L117
Hotokezaka, K., Nissanke, S., Hallinan, G., et al. 2016, ApJ, 831, 190
Hotokezaka, K., & Piran, T. 2015, MNRAS, 450, 1430
Hu, L., et al. 2017, GCN, 21883, 1
Hulse, R. A., & Taylor, J. H. 1975, ApJL, 195, L51
Hurley, K., Mitrofanov, I. G., Golovin, D., et al. 2013, in EAS Publications Series, Vol. 61, EAS Publications Series, ed. A. J. Castro-Tirado, J. Gorosabel, & I. H. Park, 459–464
Im, M., et al. 2017a, GCN, 21563, 1
—. 2017b, GCN, 21566, 1
—. 2017c, GCN, 21632, 1
—. 2017d, GCN, 21597, 1
Jin, Z.-P., Hotokezaka, K., Li, X., et al. 2016, Nature Communications, 7, 12898
Johnston, S., Bailes, M., Bartel, N., et al. 2007, PASA, 24, 174
K. Alexander et al. 2017, ApJL, *In Press*
Kalogera, V., Belczynski, K., Kim, C., O'Shaughnessy, R., & Willems, B. 2007, PhR, 442, 75
Kaplan, D., et al. 2017a, GCN, 21574, 1
—. 2017b, GCN, 21927, 1
—. 2017c, GCN, 21637, 1
Kasen, D., Badnell, N. R., & Barnes, J. 2013, ApJ, 774, 25
Kasen, D., et al. 2017, doi:DOI 10.1038/nature24453, nature, in press
Kasliwal, M., Nakar, E., Singer, L. P., & Kaplan, D. e. a. 2017, doi:10.1126/science.aap9455, science, submitted
Kilpatrick, C. D., et al. 2017, GCN, 21583, 1
Kim, S., Schulze, S., & Resmi, L. e. a. 2017, ApJL, in prep
Klebesadel, R. W., Strong, I. B., & Olson, R. A. 1973, ApJL, 182, L85
Klotz, A., et al. 2017, GCN, 21558, 1
Kocevski, D., Thöne, C. C., Ramirez-Ruiz, E., et al. 2010, MNRAS, 404, 963
Kocevski, D., et al. 2017, GCN, 21534, 1
Kouveliotou, C., Meegan, C. A., Fishman, G. J., et al. 1993, ApJL, 413, L101
Kramer, M., et al. 2017, GCN, 21920, 1
Kulkarni, S. R. 2005, ArXiv Astrophysics e-prints, astro-ph/0510256
Labanti, C., Di Cocco, G., Ferro, G., et al. 2003, A&A, 411, L149
Lattimer, J. M., & Schramm, D. N. 1974, ApJL, 192, L145
—. 1976, ApJ, 210, 549
Lee, W. H., & Ramirez-Ruiz, E. 2007, New Journal of Physics, 9, 17
Levan, A., & Tanvir, N. 2017, apJL, submitted
Levan, A., et al. 2017a, GCN, 21781, 1
—. 2017b, GCN, 21681, 1
Li, L.-X., & Paczyński, B. 1998, ApJL, 507, L59
Li, T. P., Xiong, S. L., Zhang, S. N., et al. 2017, Science China Physics, Mechanics & Astronomy, doi:10.1007/s11433-017-9107-5
Li, W., Chornock, R., Leaman, J., et al. 2011a, MNRAS, 412, 1473
Li, W., Leaman, J., Chornock, R., et al. 2011b, MNRAS, 412, 1441
Liao, J. Y., et al. 2017, GCN, 21518, 1
LIGO Scientific and Virgo Collaboration, et al. 2017
Lipunov, V., Gorbovskoy, E., & Kornilov, V. e. a. 2017, ApJL, in press
Lipunov, V., Kornilov, V., Gorbovskoy, E., et al. 2010, Advances in Astronomy, 2010, 349171
Lipunov, V., et al. 2017a, GCN, 21546, 1
—. 2017b, GCN, 21570, 1
Lipunov, V. M., Postnov, K. A., & Prokhorov, M. E. 1987, A&A, 176, L1
Lund, N., Budtz-Jørgensen, C., Westergaard, N. J., et al. 2003, A&A, 411, L231
Lyman, J., et al. 2017, GCN, 21582, 1
Lynch, C., et al. 2017a, GCN, 21670, 1
—. 2017b, GCN, 21740, 1
—. 2017c, GCN, 21628, 1
—. 2017d, GCN, 21629, 1
Malesani, D., et al. 2017a, GCN, 21591, 1
—. 2017b, GCN, 21577, 1
Margutti, R., et al. 2017, GCN, 21648, 1
Martinez-Castellanos, I., et al. 2017, GCN, 21683, 1
Massevitch, A. G., Tutukov, A. V., & Iungelson, L. R. 1976, Ap&SS, 40, 115
Matsuoka, M., Kawasaki, K., Ueno, S., et al. 2009, PASJ, 61, 999
McCully, C., et al. 2017, GCN, 21908, 1
McCully et al. 2017, ApJL, accepted
Meegan, C., Lichti, G., Bhat, P. N., et al. 2009, ApJ, 702, 791
Melandri, A., et al. 2017a, GCN, 21532, 1
—. 2017b, GCN, 21556, 1
—. 2017c, GCN, 21596, 1
Messick, C., et al. 2017, PhRvD, 95, 042001
Metzger, B. D. 2017, Living Reviews in Relativity, 20, 3
Metzger, B. D., & Berger, E. 2012, ApJ, 746, 48

Metzger, B. D., Martínez-Pinedo, G., Darbha, S., et al. 2010, MNRAS, 406, 2650
Moldon, J., Beswick, R., et al. 2017a, GCN, 21804, 1
Moldon, J., et al. 2017b, GCN, 21940, 1
Moller, A., et al. 2017, GCN, 21542, 1
Mooley, K. P., et al. 2017a, GCN, 21650, 1
—. 2017b, GCN, 21814, 1
Murphy, T., et al. 2017, GCN, 21842, 1
Nakahira, S., et al. 2017, GCN, 21641, 1
Nakaoka, T., et al. 2017, GCN, 21623, 1
Nakar, E. 2007, PhR, 442, 166
Nakar, E., & Piran, T. 2011, Nature, 478, 82
Narayan, R., Paczynski, B., & Piran, T. 1992, ApJL, 395, L83
Nicholl, M., et al. 2017a, GCN, 21541, 1
—. 2017b, GCN, 21580, 1
—. 2017c, GCN, 21585, 1
Nicholl et al. 2017, ApJL, *In Press*
Nissanke, S., Kasliwal, M., & Georgieva, A. 2013, ApJ, 767, 124
Nitz, A., et al. 2017a, ligo-cbc/pycbc: O2 Production Release 20, , , doi:10.5281/zenodo.883086. https://doi.org/10.5281/zenodo.883086
Nitz, A. H., Dent, T., Dal Canton, T., Fairhurst, S., & Brown, D. A. 2017b, arXiv:1705.01513
Ofek, E. O., Cenko, S. B., Gal-Yam, A., et al. 2007, ApJ, 662, 1129
Oppenheimer, J. R., & Volkoff, G. M. 1939, Physical Review, 55, 374
P. Cowperthwaite et al. 2017, ApJL, *In Press*
Paciesas, W. S., Meegan, C. A., von Kienlin, A., et al. 2012, ApJS, 199, 18
Paczynski, B. 1986, ApJL, 308, L43
Paragi, Z., et al. 2017a, GCN, 21763, 1
—. 2017b, GCN, 21939, 1
Pavana, M., et al. 2017, GCN, 21554, 1
Pearson, T. J., Readhead, A. C. S., et al. 2017, GCN, 21760, 1
Pian, E., DAvanzo, P., & et al. 2017, Nature in press, doi:10.1038/nature24298
Pian, E., et al. 2017, GCN, 21592, 1
Piano, G., et al. 2017, GCN, 21526, 1
Pilia, M., et al. 2017, GCN, 21525, 1
Piran, T., Nakar, E., & Rosswog, S. 2013, MNRAS, 430, 2121
Postnov, K. A., & Yungelson, L. R. 2014, Living Reviews in Relativity, 17, 3
Pozanenko, A., et al. 2017a, GCN, 21635, 1
—. 2017b, GCN, 21898, 1
—. 2017c, GCN, 21644, 1
—. 2017d, GCN, 21618, 1
Prandoni, I., Murgia, M., Tarchi, A., et al. 2017, ArXiv e-prints, arXiv:1703.09673
Pretorius, F. 2005, 95, 121101
Prochaska, J. X., Bloom, J. S., Chen, H.-W., et al. 2006, ApJ, 642, 989
R. Chornock et al. 2017, ApJL, *In Press*
R. Margutti et al. 2017, ApJL, *In Press*
Rabinowitz, D., Baltay, C., et al. 2017, GCN, 21599, 1
Resmi, L., et al. 2017, GCN, 21768, 1
Ricci, R., et al. 2017, GCN, 21900, 1
Roberts, L. F., Kasen, D., Lee, W. H., & Ramirez-Ruiz, E. 2011, ApJL, 736, L21
Rosswog, S. 2005, ApJ, 634, 1202
Sadler, E. M., et al. 2017, GCN, 21645, 1
Sathyaprakash, B. S., & Dhurandhar, S. V. 1991, PhRvD, 44, 3819
Savchenko, V., Neronov, A., & Courvoisier, T. J.-L. 2012, A&A, 541, A122
Savchenko, V., Ferrigno, C., Kuulkers, E., et al. 2017, ApJ, in press
Savchenko, V., et al. 2017a, GCN, 21507, 1
—. 2017b, GCN, 21672, 1
Schlafly, E. F., & Finkbeiner, D. P. 2011, ApJ, 737, 103
Schulze, S., et al. 2017, GCN, 21747, 1
Shapiro, S. L., & Teukolsky, S. A. 1983, Black holes, white dwarfs, and neutron stars: The physics of compact objects
Shappee et al. 2017, Science, doi:10.1126/science.aaq0186
Shara, M., et al. 2017, GCN, 21610, 1
Shklovsky, I. S. 1967, ApJL, 148, L1
Siebert et al. 2017, ApJL submitted
Simon, J. D., et al. 2017, GCN, 21551, 1
Singer, L. P., & Price, L. 2016, PhRvD, 93, 024013
Singer, L. P., et al. 2016, arXiv:1603.07333
—. 2017a, GCN, 21552, 1
—. 2017b, GCN, 21779, 1
—. 2017c, GCN, 21569, 1
Singh, K. P., Tandon, S. N., Agrawal, P. C., et al. 2014, ASTROSAT mission, , , doi:10.1117/12.2062667. http://dx.doi.org/10.1117/12.2062667
Smartt et al. 2017, Nature in press
Soderberg, A. M., Berger, E., Kasliwal, M., et al. 2006, ApJ, 650, 261
Sugita, S., Kawai, N., Negoro, H., et al. in prep., PASJ
Sugita, S., et al. 2017, GCN, 21555, 1
Svinkin, D., Hurley, K., von, K. A., et al. 2017, GRB Coordinates Network, 21515
Svinkin, D., et al. 2017a, GCN, 21746, 1
—. 2017b, GCN, 21515, 1
Swarup, G., Ananthakrishnan, S., Kapahi, V. K., et al. 1991, Current Science, 60, 95. http://www.jstor.org/stable/24094934
Tanaka, M. 2016, Advances in Astronomy, 2016, 634197
Tanaka, M., & Hotokezaka, K. 2013, ApJ, 775, 113
Tanvir, N., & Levan, A. 2017, apJL, accepted

Tanvir, N. R., Levan, A. J., Fruchter, A. S., et al. 2013, Nature, 500, 547
Tanvir, N. R., et al. 2017a, GCN, 21544, 1
—. 2017b, GCN, 21576, 1
Tavani, M., Barbiellini, G., Argan, A., et al. 2009, A&A, 502, 995
Taylor, J. H., & Weisberg, J. M. 1982, Astrophys. J., 253, 908
Taylor, J. H., Wolszczan, A., Damour, T., & Weisberg, J. M. 1992, Nature, 355, 132
The LIGO Scientific Collaboration, The Virgo Collaboration, et al. 2017a, GCN, 21505, 1
—. 2017b, GCN, 21513, 1
—. 2017c, GCN, 21527, 1
—. 2017d, An estimate of the Hubble constant from the first joint gravitational wave and electromagnetic observation of a binary neutron star merger, Tech. rep. https://git.ligo.org/publications/gw170817/h0-inference
—. 2017e, Discovery of a Short Gamma-Ray Burst Associated with a Binary Neutron Star Merger, Tech. rep. https://git.ligo.org/publications/gw170817/gw-grb170817
—. 2017f, GCN, 21509, 1
—. 2017g, GCN, 21510, 1
Tingay, S. J., Goeke, R., Bowman, J. D., et al. 2013, PASA, 30, e007
Tominaga, et al. 2017, GCN, 21595, 1
Tonry, J., et al. 2017, GCN, 21886, 1
Troja, E., King, A. R., O'Brien, P. T., Lyons, N., & Cusumano, G. 2008, MNRAS, 385, L10
Troja, E., Sakamoto, T., Cenko, S. B., et al. 2016, ApJ, 827, 102
Troja, E., et al. 2017a, GCN, 21682, 1
—. 2017b, GCN, 21778, 1
Troja, E., Piro, L., van Eerten, H., et al. 2017, Nature, doi:10.1038/nature24290
Troja, E., et al. 2017a, GCN, 21765, 1
—. 2017b, GCN, 21787, 1
—. 2017c, GCN, 21803, 1
Tunnicliffe, R. L., Levan, A. J., Tanvir, N. R., et al. 2014, MNRAS, 437, 1495
Ubertini, P., Lebrun, F., di Cocco, G., et al. 2003, A&A, 411, L131
Valenti, S., et al. 2017, GCN, 21606, 1
van Haarlem, M. P., Wise, M. W., Gunst, A. W., et al. 2013, A&A, 556, A2
Vedrenne, G., Roques, J.-P., Schönfelder, V., et al. 2003, \aap, 411, L63
Veitch, J., Raymond, V., Farr, B., et al. 2015, Phys. Rev. D, 91, 042003. http://link.aps.org/doi/10.1103/PhysRevD.91.042003
Verrecchia, F., et al. 2017, GCN, 21785, 1
Verrecchia, V., et al. 2017, in prep.
Villasenor, J. S., Lamb, D. Q., Ricker, G. R., et al. 2005, Nature, 437, 855
V.M.Lipunov. 2017, GCN, 21621, 1
V.M.Lipunov, et al. 2017a, GCN, 21687, 1
—. 2017b, GCN, 21587, 1
von Kienlin, A., Meegan, C., Goldstein, A., et al. 2017, GCN, 21520, 1
von Kienlin, A., Beckmann, V., Rau, A., et al. 2003, A&A, 411, L299
Wex, N. 2014, arXiv:1402.5594
White, D. J., Daw, E., & Dhillon, V. 2011, Classical and Quantum Gravity, 28, 085016
White, D. J., Daw, E. J., & Dhillon, V. S. 2011, Classical and Quantum Gravity, 28, 085016
Wieringa, M., et al. 2017, GCN, 21882, 1
Wiersema, K., et al. 2017, GCN, 21594, 1
Williams, P. K. G., et al. 2017a, GCN, 21750, 1
—. 2017b, GCN, 21571, 1
Wilson, W. E., Ferris, R. H., Axtens, P., et al. 2011, MNRAS, 416, 832
Wilson-Hodge, C. A., Case, G. L., Cherry, M. L., et al. 2012, ApJS, 201, 33
Winkler, C., Courvoisier, T. J.-L., Di Cocco, G., et al. 2003, A&A, 411, L1
Wiseman, P., et al. 2017, GCN, 21584, 1
Wolf, C., et al. 2017, GCN, 21560, 1
Wootten, A., & Thompson, A. R. 2009, IEEE Proceedings, 97, 1463
Yang, S., et al. 2017a, GCN, 21531, 1
—. 2017b, GCN, 21579, 1
—. 2017c, GCN, 21539, 1
Yoshida, et al. 2017a, GCN, 21549, 1
—. 2017b, GCN, 21561, 1
—. 2017c, GCN, 21586, 1
—. 2017d, GCN, 21685, 1
Yu, P.-C., et al. 2017, GCN, 21669, 1
Zadrożny, A., Sokołowski, M., Mankiewicz, L., & Żarnecki, A. F. 2017, Pi of the Sky in LSC-Virgo's EM follow-up in O1 science run, , , doi:10.1117/12.2281024. http://dx.doi.org/10.1117/12.2281024